

# Tight-binding model describes frontier orbitals of nonfullerene acceptors

Journal:	Molecular Systems Design & Engineering
Manuscript ID	ME-ART-12-2023-000195
Article Type:	Paper
Date Submitted by the Author:	16-Dec-2023
Complete List of Authors:	Jindal, Vishal; Penn State University, Chemical Engineering Janik, Michael; Penn State University, Chemical Engineering Milner, Scott; Penn State University, Chemical Engineering

SCHOLARONE™ Manuscripts

# Design, System, Application

The active layer of organic photovoltaics blends electron acceptor and donor materials, comprising organic small molecules and conjugated polymers. Donor and acceptor frontier molecular orbitals dictate their charge transfer characteristics. The modularity in the molecular design of recently developed nonfullerene acceptors allows for a tunable molecular structure and has propelled the power conversion efficiency of organic photovoltaics to exceed 19%. Conjugated aromatic units of the acceptor backbone can be systematically varied to evaluate substituent effects on frontier molecular orbitals. In this work, we develop a tightbinding electronic structure approach to connect  $\pi$ -conjugated frontier orbitals to the orbital properties and interactions among the individual conjugated moieties in acceptor molecules. Our approach combines theory and simulations to calculate the energies and wavefunctions of the frontier orbitals. We demonstrate that the parameters fitted to model homo-oligomers and alternating co-oligomers effectively represent the electronic structure for 'hetero oligomer' non-fullerene acceptors. Our results illustrate how a tight-binding model reduces the electronic degrees of freedom to provide a computationally efficient method for modeling the electronic structure across compositions and structures of non-fullerene acceptors.

# Tight-binding model describes frontier orbitals of non-fullerene acceptors

Vishal Jindal, Michael J. Janik, Scott T. Milner

Department of Chemical Engineering

The Pennsylvania State University, University Park, PA, 16801, USA

#### Abstract

Optoelectronic properties of organic photovoltaics, including light absorption, intramolecular and intermolecular charge transfer, depend on the energetics of the frontier molecular orbitals of constituent organic materials. We develop a tight-binding model for an indacenodithiophene-based small molecule non-fullerene acceptor - IDTBR, which gives a high-efficiency organic photovoltaic cell in combination with poly(3-hexylthiophene) as donor. By choosing stiff conjugated ring moieties as sites, we obtain tight-binding parameters that are local to each moiety, and transferable to other chain architectures. In particular, parameters from homo-oligomers and alternating co-oligomers of constituent moieties can be used, without adjustment, to define the tight-binding model for IDTBR, which reasonably predicts the energies and wavefunctions of its frontier molecular orbitals. Transferability of model parameters will enable efficient screening and selection of molecular architectures with desirable optoelectronic properties.

# 1 Introduction

Organic photovoltaics (OPVs) show promise as a flexible alternative to hard material-based photovoltaics. [1] High-efficiency OPVs employ non-fullerene acceptors, which are conjugated hetero-oligomers, together with conjugated polymers as donors. [2, 3, 4, 5, 6] The molecular architecture of non-fullerene acceptors can be tuned for optimal optoelectronic and structural properties. [7, 8, 9] By perturbing the core and side chains of acceptors, their propensity to crystallize and miscibility with donor polymers can be tuned. [10] Donor-acceptor miscibility plays a crucial role in determining the active layer morphology, and can be exploited to design efficient organic photovoltaics. [11]

Many conjugated architectures have been proposed as non-fullerene acceptors, but synthesis and testing of each new candidate molecule is slow and costly. [12, 13, 14, 15] Improved theoretical and computational techniques for exploring the structure-property relationships of these molecules could accelerate material design. [10, 16] In principle, quantum mechanical calculations using density functional theory (DFT) can predict optoelectronic properties such as optical gap and exciton structure for non-fullerene acceptors and donor-acceptor interfaces. Indeed, DFT and classical molecular dynamic simulations have been combined to investigate the microstructure and electron transport properties of conjugated organic systems. [17] However, using DFT to predict electronic properties of disordered systems is challenging because of the lack of periodicity, and need to average over nanoscale disorder.

Tight binding models provide a semi-empirical description of the electronic structure of conjugated molecules and polymers using constituent aromatic moieties or "rings" as building blocks. These rings are planar, stiff and tightly coupled electronically, which makes them appropriate units for coarse-graining. The flexible dihedrals influence the inter-ring hopping terms, which vary as the cosine of the dihedral angles and allow for delocalization of charge along the conjugated backbone. [18] Tight-binding model have successfully described the conduction and valence bands of homopolymer organic semiconductors. [19, 18] For instance, for an infinite chain of poly(3-hexylthiophene) (P3HT), these models can accurately predict the effects of dihedral disorder on absorption spectra [18]; the structure of excitons in bulk and at donor-acceptor interfaces [20]; polaron formation mechanisms [21]; and polaron hopping barriers and rates. [22] Recently, we used tight-binding parameters derived from DFT calculations on constituent homopolymers to accurately predict the frontier molecular orbitals of alternating copolymers demonstrating transferability of parameters from one chain architecture to another. [23]

In a previous study, Zwijnenburg et al. [24] used density functional tight-binding methods (DFTB) [25, 26, 27, 28, 29], based on the GFN-xTB approach [26], to computationally screen optoelectronic properties of various conjugated donor-acceptor polymers. Semi-empirical quantum mechanical methods such as DFTB or GFN-xTB are atomistic calculations, derived from a DFT perturbation expansion of the electron density in fluctuation terms to various orders. DFTB calculations are suited for large systems of more than 1000 atoms for a variety of chemical systems and applications. Such calculations are 2-3 orders of magnitude faster than DFT, but generally require parameters to be determined for all pair of atoms present, as a function of interatomic distances.

Long-chain polymers can be effectively modeled using periodic boundary conditions, and tight-binding parameters can be determined through band structure calculations. [18, 23] In contrast, non-fullerene acceptors

(NFAs) are oligomers consisting of hetero aromatic monomers. Troisi et al. proposed a computational screening approach to identify novel small-molecule NFAs with targeted electronic properties (orbitals energies, excited state energies, and oscillator strength), solubility, and reorganization energy for chemical reduction by modification of known organic semiconductors derived from the Cambridge Structural Database.[16]

Here, we use frontier orbital energies and wavefunctions from DFT calculations on constituent moieties to predict the frontier orbitals of non-fullerene acceptors. A single choice of parameters for constituent moieties gives accurate results for different geometries, and each individual calculation of parameters is quite fast. This allows for frontier orbital calculation on non-fullerene acceptors which is 10<sup>6</sup> times faster than full DFT calculation. We can treat excitons and polarons on non-fullerene acceptors by building from this basic approach, and predict polaron mobility along disordered chains, as well as Marcus hopping of polarons between chains, both of which will be presented in future publications.

Recently, our group developed efficient molecular dynamic (MD) simulations based on virtual sites to equilibrate configurations of conjugated molecules in bulk and at donor-acceptor interfaces [30]. The ensemble of configurations from these fast MD simulations can be used in conjunction with tight-binding models to average over dihedral disorder and predict optoelectronic properties of bulk phases and donor-acceptor interfaces. As a next step in this program, in this paper we extend the tight-binding approach to describe charge carriers on a non-fullerene acceptor, IDTBR. [2] IDTBR (Fig. 1) is made up of four different monomers which are commonly used OPV materials: phenylene, thiophene, benzothiadiazole, and rhodanine. The central indacenodithiophene moiety consists of two thiophene rings bridged onto a phenyl ring, which form an electron-rich core. This core is flanked on either side by electron-withdrawing groups, benzothiadiazole and (3-ethyl)rhodanine.

Figure 1: IDTBR molecular structure

Similar to IDTBR, other non-fullerene acceptors also consist of different electron-rich and electron-withdrawing moieties. The presence of many moieties poses an interesting computational challenge, as multiple parameters are required to describe a tight-binding model for charge carriers on these hetero-oligomers.

To assign these parameters, we match the HOMO and LUMO levels from the tight-binding model to DFT results for a series of homo-oligomers and alternating co-oligomers. On physical grounds, we expect tight-binding parameters to be local and transferable, because orbital overlap between non-neighboring sites is negligible, so charges can hop only between immediate neighbors. One part of the molecular frontier wavefunction is not directly affected by distant parts of the molecule, but only through a succession of local hopping matrix elements. Consequently, parameters for a given moiety can be used in tight-binding models for hetero-oligomers and different geometries.

Previously, Mesta et al. [31] have defined tight-binding models for donor-acceptor alternating polymers using onsite energies determined from the HOMO and LUMO energy levels of constituent monomers, and hopping terms derived from the energy levels of co-dimers of those monomers. Here, we fit the onsite energies of the constituent monomers using the HOMO and LUMO energies for varying length of homo-oligomers; hopping terms are fitted using the HOMO and LUMO energies of alternating co-oligomers.

This paper is organized as follows. First, we define a tight-binding model for IDTBR. Then, we develop tight-binding model parameters for homo-oligomers and alternating co-oligomers by fitting onsite energies and hopping terms to DFT results. We explore the consequences of the dihedral angle dependence of hopping matrix elements. We transfer the tight-binding parameters derived from homo-oligomers and alternating co-oligomers of constituents monomers to IDTBR. To validate the resulting IDTBR model, tight-binding predictions for frontier orbital energies and wavefunctions are compared to DFT calculations.

Becasue tight-binding models are assembled form local, transferable parts, molecular architectures can be modified without starting over from sctratch. We demonstrate this useful aspect by modifying our model for IDTBR to describe 4F-IDTBR: an IDTBR molecule in which both benzothiadiazole moieties are doubly fluorinated, and by rotating one of the inter-ring dihedral angle of IDTBR to introduce dihedral distortions.

# 2 Methods

The tight-binding model is a semi-empirical coarse-graining approach to predict the electronic properties of conjugated organic semiconductors. Electronic degrees of freedom are drastically reduced to only a few local orbitals per site. In a tight-binding model, an electron or hole occupies sites corresponding to monomer units, and delocalizes by hopping to neighboring sites. Sites are described in terms of the local frontier orbitals of the constituent aromatic moieties. These moieties are geometrically rigid and tightly coupled

electronically, such that their internal electronic structure is only weakly perturbed by the overall chain conformation.

The parameters for the tight-binding model consist of onsite energies ( $\epsilon$ ) for charge carriers to occupy a site, and hopping matrix elements (t) that allow hopping of charge carriers from one site to an adjacent site. The hopping matrix element between sites originates physically in the orbital overlap between frontier orbitals on adjacent moieties, and is taken to be proportional to the cosine of dihedral angle between the sites. [18]

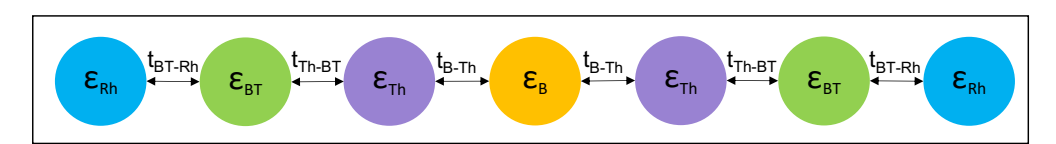


Figure 2: Schematic for the tight-binding model for IDTBR. (B - Benzene, T - Thiophene, BT - Benzothia-diazole, Rh - Rhodanine)

The IDTBR molecule is modeled as a one-dimensional array of seven sites. Fig. 2 shows the tight-binding representation for IDTBR, where each constituent monomer is modeled as a site with an onsite energy  $\{\epsilon_k\}$ . Sites are coupled to each other through hopping matrix elements denoted by  $t_{B-Th}$ ,  $t_{Th-BT}$  and  $t_{BT-Rh}$ . The tight-binding Hamiltonian takes the form:

$$H = \sum_{k=1}^{7} \epsilon_k c_k^{\dagger} c_k - \sum_{k=1}^{6} t_k \left( c_k^{\dagger} c_{k+1} + c_{k+1}^{\dagger} c_k \right) \tag{1}$$

where  $c_k^{\dagger}$  and  $c_k$  are the creation and annihilation operators of a charge carrier on site k;  $\epsilon_k$  is the onsite energy of a carrier on site k; and  $t_k$  is the hopping matrix element between sites k and k+1. The first term in Eq. 1 accounts for the energy of a charge carrier to occupy any particular site k and the second term accounts for reduction in energy due to delocalization of a carrier between  $k^{th}$  and  $k+1^{th}$  site.

In the tight-binding approximation, hopping between localized orbitals is restricted to nearest neighbors. Correspondingly, the Hamiltonian matrix is tri-diagonal with the onsite energies  $\{\epsilon_k\}$  as diagonal terms, and the hopping matrix elements  $\{t_k\}$  as off-diagonal terms. For the planar IDTBR, the tight-binding

Hamiltonian H takes the form:

$$\mathbf{H} = \begin{bmatrix} \epsilon_{Rh} & t_{BT-Rh} & 0 & 0 & 0 & 0 & 0 \\ t_{BT-Rh} & \epsilon_{BT} & t_{Th-BT} & 0 & 0 & 0 & 0 \\ 0 & t_{Th-BT} & \epsilon_{T} & t_{B-Th} & 0 & 0 & 0 \\ 0 & 0 & t_{B-Th} & \epsilon_{B} & t_{B-Th} & 0 & 0 \\ 0 & 0 & 0 & t_{B-Th} & \epsilon_{T} & t_{Th-BT} & 0 \\ 0 & 0 & 0 & 0 & t_{Th-BT} & \epsilon_{BT} & t_{BT-Rh} \\ 0 & 0 & 0 & 0 & 0 & t_{BT-Rh} & \epsilon_{Rh} \end{bmatrix}$$

$$(2)$$

where diagonal terms  $\epsilon_B$ ,  $\epsilon_T$ ,  $\epsilon_{BT}$  and  $\epsilon_{Rh}$  are the onsite energy of benzene, thiophene, benzothiadiazole and rhodanine, and  $t_{B-Th}$ ,  $t_{Th-BT}$  and  $t_{BT-Rh}$  are the hopping matrix elements between planar benzene-thiophene, thiophene-benzothiadiazole(BT), and BT-rhodanine. The energy eigenstates  $E_n$  and associated wave functions  $\Psi_n$  are obtained by solving the time-independent Schrodinger equation,  $H\Psi_n = E_n\Psi_n$ .

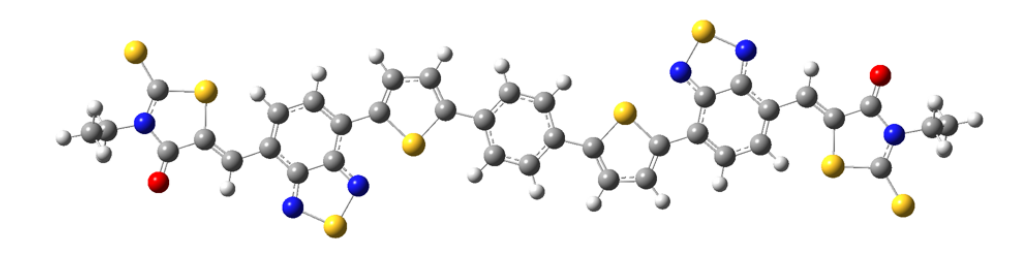
We observe that the IDTBR HOMO and LUMO wavefunctions (Fig. 3) resemble a weighted sum of the HOMOs and LUMOs of individual monomers (Fig. 4), respectively. Correspondingly, we write the IDTBR orbital wavefunction,  $\Psi$ , as a linear combination of localized molecular orbitals,  $\{\psi_k\}$ , of constituent monomers.

$$\Psi = \sum_{k=1}^{7} a_k \psi_k \tag{3}$$

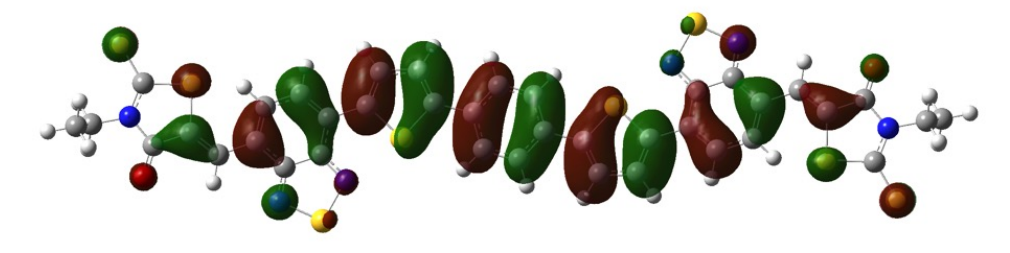
where  $a_k$  is the onsite amplitude and  $\psi_k$  is the localized frontier orbital on the  $k^{th}$  monomer. We write separate tight-binding Hamiltonians for IDTBR HOMO and LUMO, in which the constituent local orbitals are respectively the HOMOs and LUMOs of the constituent monomers. Note that we remove the alkyl (R) groups and the bridge between thiophene and phenyl rings because the side groups are electronically unimportant and do not influence the backbone conjugation.

We determine our tight-binding parameters, which are the onsite energies ( $\epsilon_B$ ,  $\epsilon_T$ ,  $\epsilon_{BT}$ ,  $\epsilon_{Rh}$ ) and the hopping matrix elements ( $t_{B-Th}$ ,  $t_{Th-BT}$ ,  $t_{BT-Rh}$ ), by fitting the HOMO and LUMO energies of oligomers of the constituent monomers to DFT results. Only homo- and co-oligomers need to be considered; the onsite energy for a constituent monomer and hopping between two such monomers can be fitted to DFT results for homo-oligomers, and hopping matrix elements between two different monomers can be determined by fitting to DFT results for alternating co-oligomers.

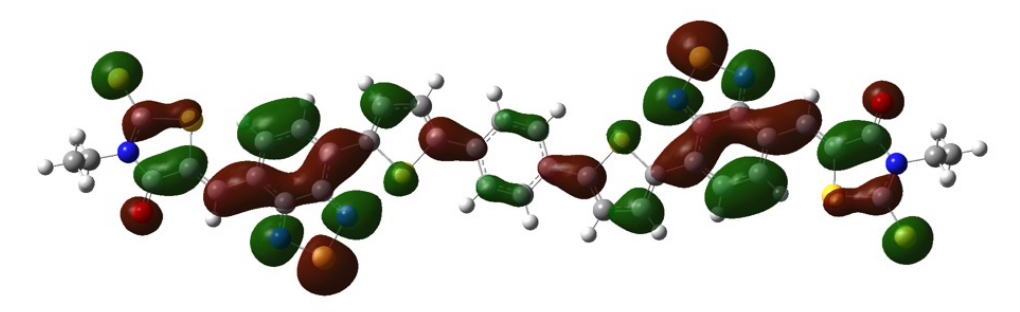
In pursuing this approach, we assume that tight-binding parameters are local and transferable. Locality



(a) IDTBR molecule [ N - blue, S - yellow, O - red, C - grey, H - white ]



(b) Highest occupied molecular orbital (HOMO) for IDTBR



(c) Lowest unoccupied molecular orbital (LUMO) for IDTBR

Figure 3: HOMO (b) and LUMO (c) for IDTBR using DFT calculations, with B3LYP functional and 6-311g(d) basis set, implemented using Gaussian 16. Iso-value of 0.01 is used to plot orbital surfaces using Gauss View 6.

of tight-binding parameters means that the parameters depend only on a site and its nearest neighbours. The onsite energy is local to a site and the hopping matrix element is local to the two adjacent sites. If the parameters are local, we can transfer the parameters obtained from homo-oligomers and co-oligomers to heterogeneous oligomers.

To validate our approach, we compare the energies and wavefunctions of IDTBR frontier molecular orbitals predicted using the tight-binding model with DFT results. To extract onsite amplitudes  $\{b_k\}$  from the DFT wavefunction, we use an orbital projection method. [32] Onsite amplitudes can be calculated by projecting the

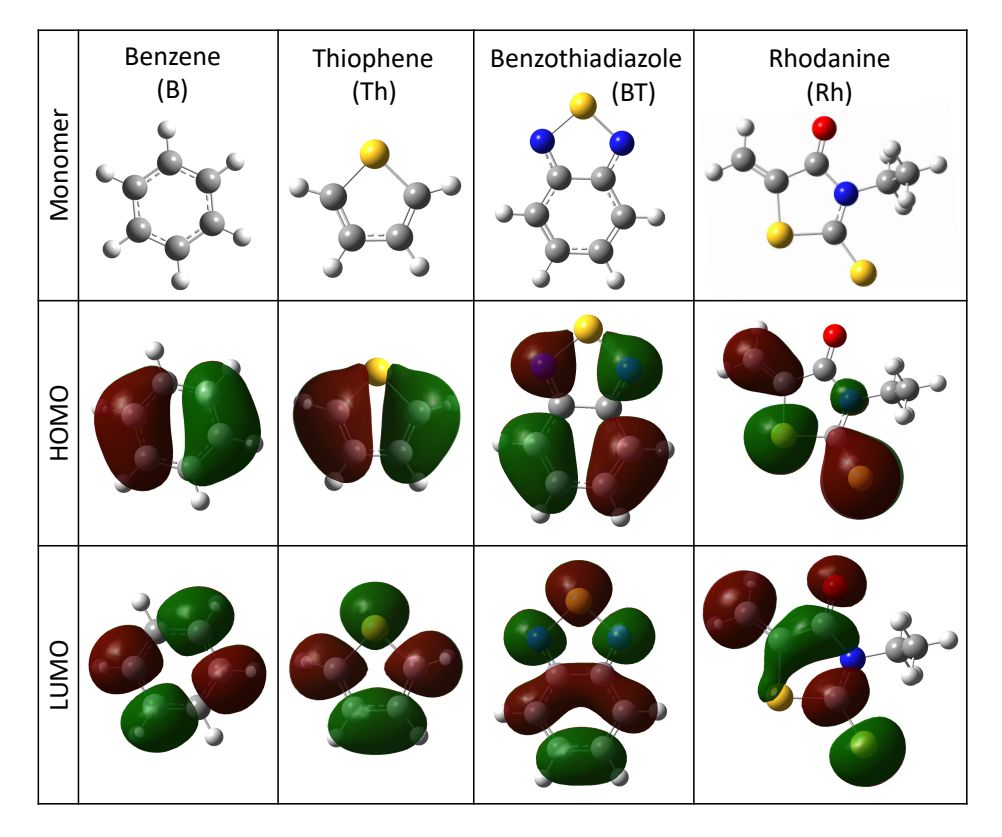


Figure 4: Constituent monomers and their HOMO, LUMO wavefunctions.

localized molecular orbital of a constituent monomer onto the molecular orbital of the entire molecule:

$$b_k = <\Psi_{molecule}|\psi_k> \tag{4}$$

here,  $b_k$  is the onsite amplitude for site k,  $\psi_k$  is a localized molecular orbital on monomer at site k, and  $\Psi_{molecule}$  is a molecular orbital on the entire molecule. These projections can be calculated numerically, by using cube files generated from DFT packages. To test the tight-binding approach, the onsite amplitudes predicted using the tight-binding model  $\{a_k\}$  are compared to the onsite projections  $\{b_k\}$  extracted from DFT orbitals for oligomers.

# 3 TBM parameters from oligomers

Density functional theory (DFT) calculations are used to fix parameters for tight-binding models of homooligomers and alternating co-oligomers of varying lengths made from the constituent monomers of IDTBR (benzene, thiophene, benzothiadiazole, and rhodanine), by fitting to the HOMO and LUMO energy versus oligomer length. For rhodanine, we used the DFT HOMO or LUMO energy of the monomer as the respective onsite energy.

This procedure also serves as a test of model assumptions: that a single frontier orbital per monomer suffices to represent the frontier orbital of the oligomer, and that the onsite energies and the hopping matrix elements are effectively constants independent of bonded neighbors or hydrogen termination. By comparing tight-binding model predictions with DFT results, we can test the validity of these approximations and identify where modifications are necessary.

DFT calculations are performed within Gaussian 16 using the hybrid functional B3LYP [33, 34, 35, 36] with 6-311g(d) basis set. The optimized monomer geometries are assembled into oligomers using GaussView 6 by replacing the appropriate hydrogen on a monomer with another monomer and so on, without further geometry optimization. Dihedral angles are then set to give planar, all-trans configurations. For IDTBR and thiophene pentamer, we tested that the total energy in the sticking together and optimized molecule differs by less than 0.1 eV.

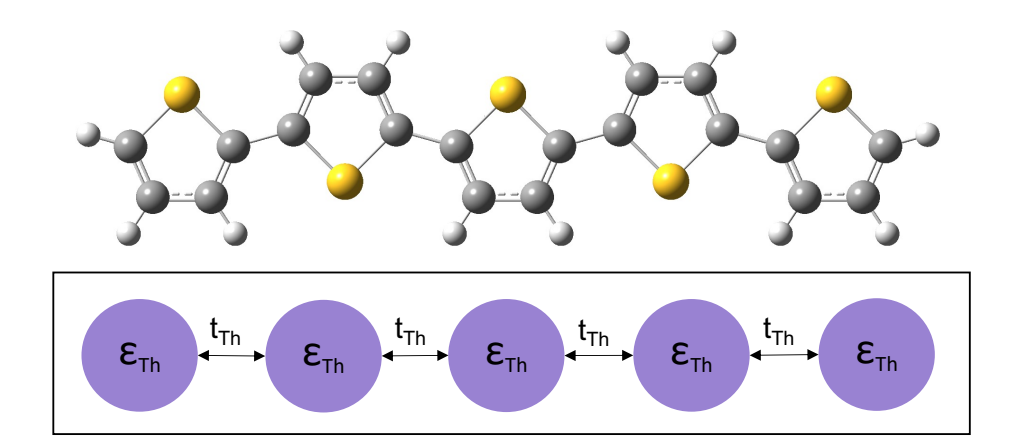


Figure 5: Tight-binding model for thiophene homo-oligomer (pentamer).

Fig. 5 shows a tight-binding model for a thiophene homo-oligomer consisting of five thiophene rings. There are two sets of onsite energies and hopping matrix elements, one each for HOMO and LUMO of the oligomer. We use the same onsite energy and hopping matrix element throughout the homo-oligomer chain. Similarly, tight-binding models can be formulated for homo-oligomers of different lengths and consisting of a different monomer of interest.

Tight-binding predictions for the HOMO and LUMO energies versus oligomer length are fitted to DFT results by adjusting the onsite energy ( $e_H$  for HOMO,  $e_L$  for LUMO) and hopping matrix element ( $t_H$  for HOMO,  $t_L$  for LUMO). Fig. 6 compares HOMO and LUMO energies from DFT with tight-binding predictions for oligothiophenes.

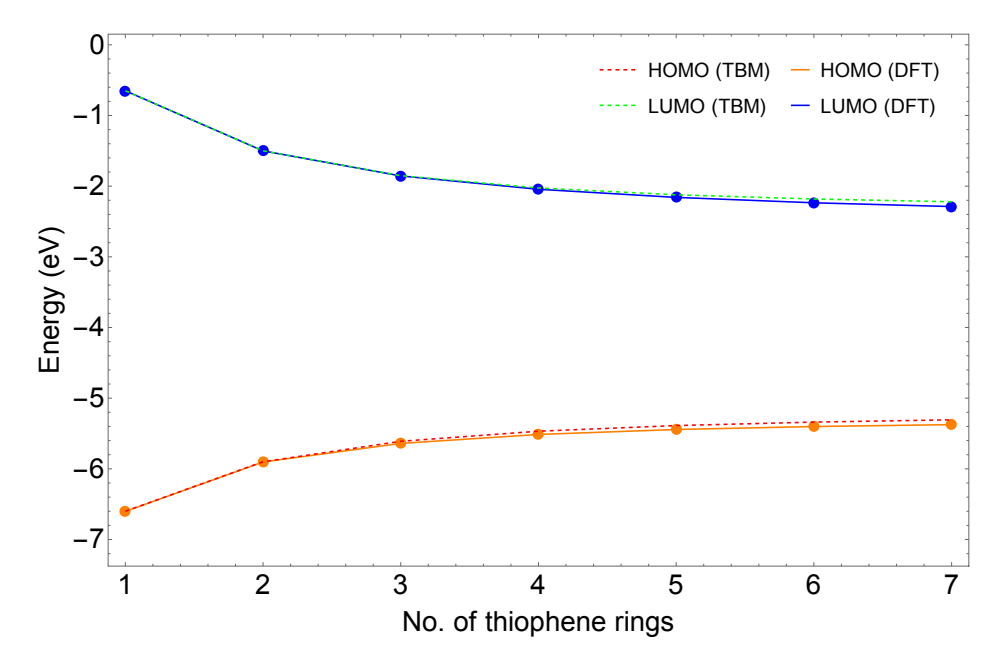


Figure 6: HOMO (orange points) and LUMO (blue points) energy (in eV) from DFT calculations on oligothiophenes, compared to tight-binding predictions with fitted parameters (red and green dashed curves).

Table 1: Tight binding parameters (in eV) for thiophene, benzene, and benzothiadiazole homo-oligomers. Onsite energies for rhodanine are DFT HOMO, LUMO energies.

Monomer	$e_H$	$t_H$	$e_L$	$t_L$
Thiophene	-6.60	-0.70	-0.65	0.85
Phenylene	-6.90	-0.73	-0.30	0.80
Benzothiadiazole	-6.80	-0.47	-2.90	0.38
Rhodanine	-6.89	-	-2.86	-

Table 1 lists the onsite energies of thiophene, benzene, benzothiadiazole and rhodanine. For all three homooligomers, the tight-binding theory gives a quantitative account of the HOMO and LUMO energy levels versus oligomer length, with a single set of parameters that works even for the monomer.

We can further validate the tight-binding model by comparing predicted HOMO and LUMO wavefunctions to onsite amplitudes extracted from DFT orbitals. Fig. 7 makes that comparison for thiophene pentamer. The tight-binding model prediction for the HOMO wavefunction amplitudes matches the normalized DFT-derived projection results. For the LUMO, the prediction accurately matches the DFT results as well.

The oligomer HOMO is formed from anti-bonding interactions between the HOMO on each thiophene ring and the LUMO is formed from bonding interactions between the LUMO on each ring. We solve the tight-binding Hamiltonian analytically to compute frontier orbital energy  $E_k$  and wavefunction  $\Psi_k$  for homo-

oligomers and alternating co-oligomers (see appendix). For homo-oligomer of length n,

$$E_k = \epsilon - 2t \cos k \tag{5}$$

where  $k = \pi/(n+1)$  and  $k = n\pi/(n+1)$  for the maximally bonding and anti-bonding states. Correspondingly, the lowest eigenvector  $\psi_1$  of the Hamiltonian matrix is

$$\psi_1(j) = \sqrt{2/(n+1)}\sin(\pi j/(n+1)) \tag{6}$$

in which j runs over the site indices 1, ... n, vanishing at the "phantom sites" just beyond the ends of the oligomer, at j = 0 and j = n + 1. The highest eigenvector  $\psi_n$  is the same sine function, but with a sign change between every pair of adjacent sites:

$$\psi_n(j) = (-1)^j \sqrt{2/(n+1)} \sin(\pi j/(n+1)) \tag{7}$$

The HOMO and LUMO wavefunctions calculated using DFT have the expected form, of the corresponding HOMO and LUMO on the monomer, modulated with a qualitatively sinusoidal envelope function (see orbital images of Fig. 7).

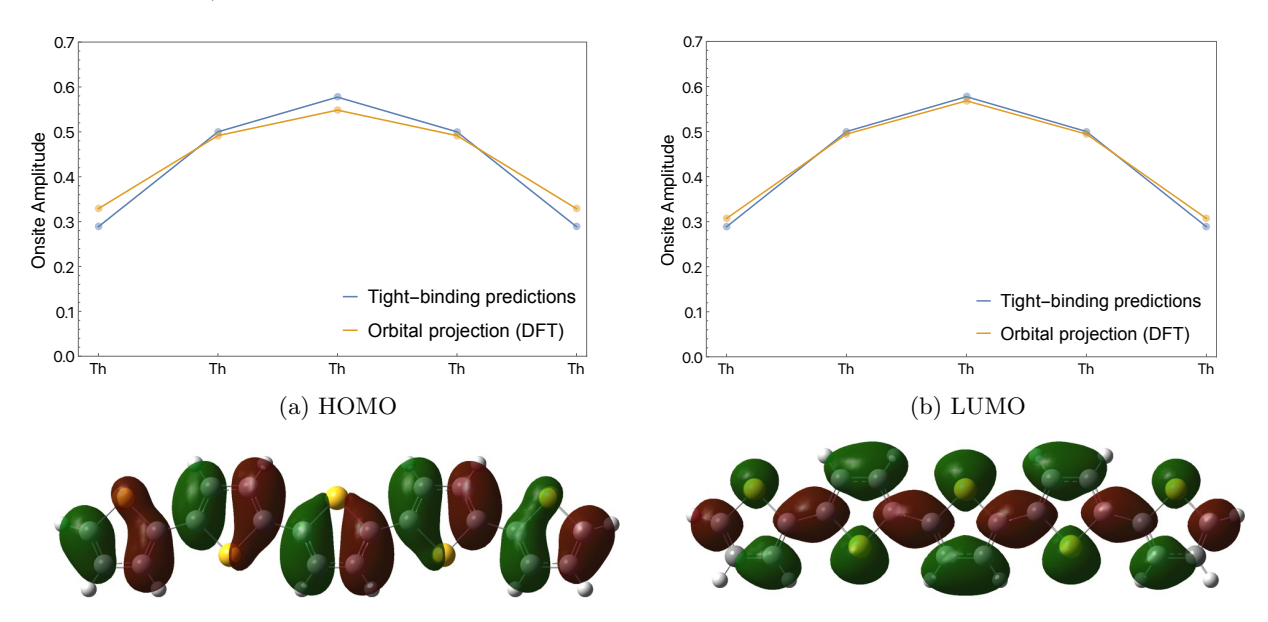


Figure 7: Onsite amplitudes of HOMO (a) and LUMO (b) wavefunction obtained using orbital projection of DFT results (orange), compared to tight-binding prediction (blue) for thiophene pentamer. At the bottom are the corresponding orbital images from Gaussian. An iso-value of 0.01 is used for orbital surfaces.

We repeat the process of matching the HOMO and LUMO energies from a tight-binding model to DFT results

for varying lengths of co-oligomers to fit hopping matrix elements between different monomers. Like our DFT calculations for homo-oligomers, optimized monomer geometries are assembled into co-oligomers without further optimization, and dihedral angles are set to give planar, symmetric configurations. By this procedure, we can check whether onsite energies fitted to homo-oligomers are transferable to co-oligomers.

Fig. 8 shows a tight-binding model for thiophene-BT alternating co-oligomer consisting of five rings. Similar models can be defined for co-oligomers of different length of co-monomers. As the coupling is between the same pair of monomers, we use a single hopping matrix element ( $t_{Th-BT}$  in the case of thiophene-BT alternating co-oligomer) to define a tight-binding model for an alternating co-oligomer. Fig. 9 compares tight-binding predicted HOMO and LUMO energies with DFT results for thiophene-BT alternating co-oligomers. Tight-binding predicted energies fit very well to DFT; this validates the transferability of onsite energies to alternating co-oligomers.

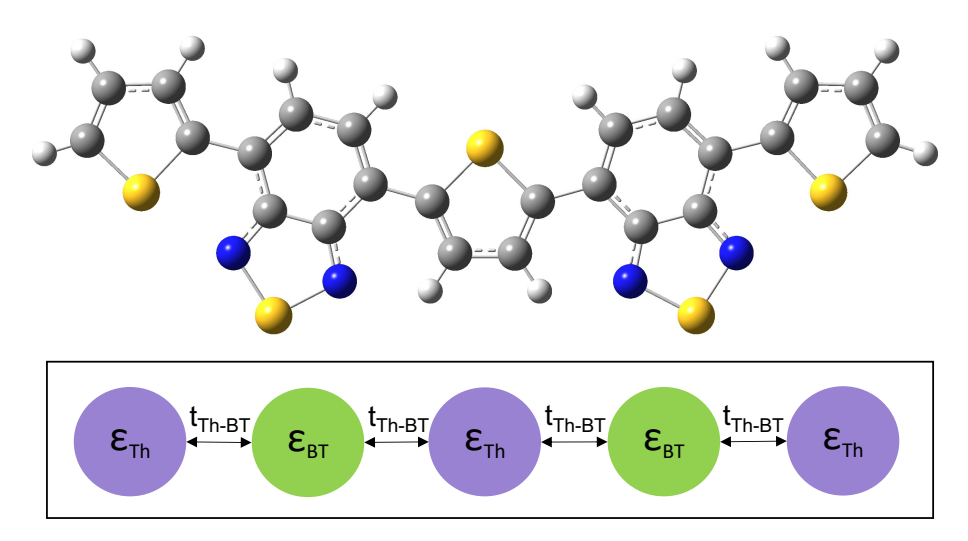


Figure 8: Tight-binding model of alternating co-oligomer for thiophene - benzothiadiazole consisting of five monomer rings.

We use HOMO and LUMO energies of BT-Rh dimer to fit  $t_{BT-Rh}$ . For rhodanine, the HOMO-1 is the relevant frontier orbital; the rhodanine HOMO is a non-bonding isolated state, whereas the rhodadine HOMO-1 hybridizes with the BT HOMO to produce oligomer HOMO states.

Fig. 10 shows that the HOMO and LUMO wavefunctions predicted using the tight-binding model compare well to onsite amplitudes extracted from DFT results for a thiophene-BT pentamer. We observe a larger deviation in the predicted HOMO wavefunction at the edge of the molecule compared to DFT results. The HOMO onsite amplitudes nearly follow sinusoidal oscillations similar to a particle in a box, while the modulated sinusoidal nature of the LUMO depict substantial push-pull effect because of different onsite

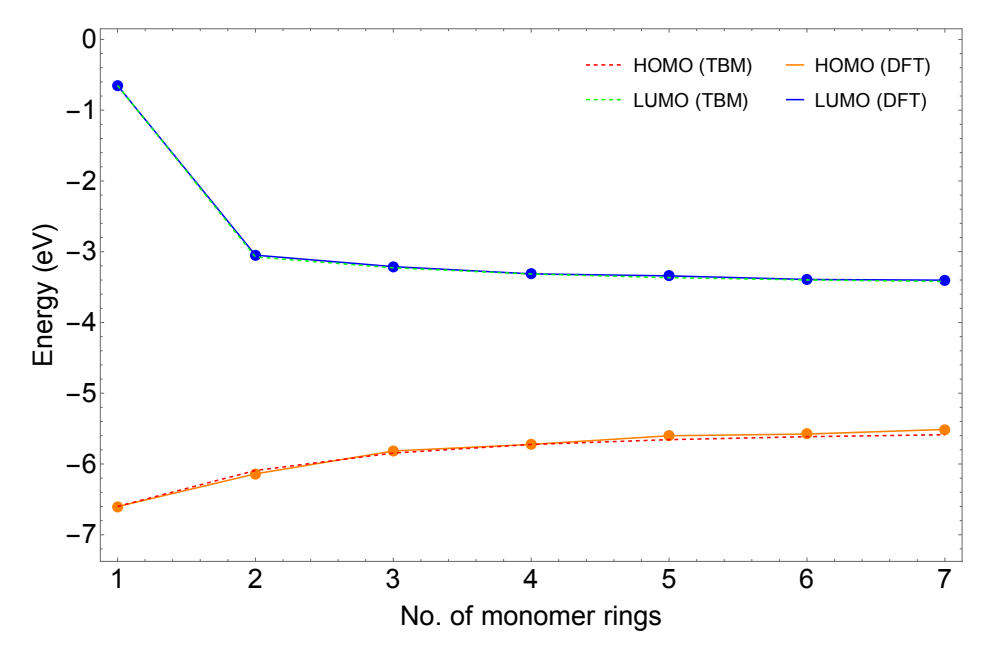


Figure 9: HOMO (orange points) and LUMO (blue points) energy (in eV) from DFT calculations on thiophene-BT alternating co-oligomers, compared to tight-binding predictions with fitted parameters (red and green dashed curves).

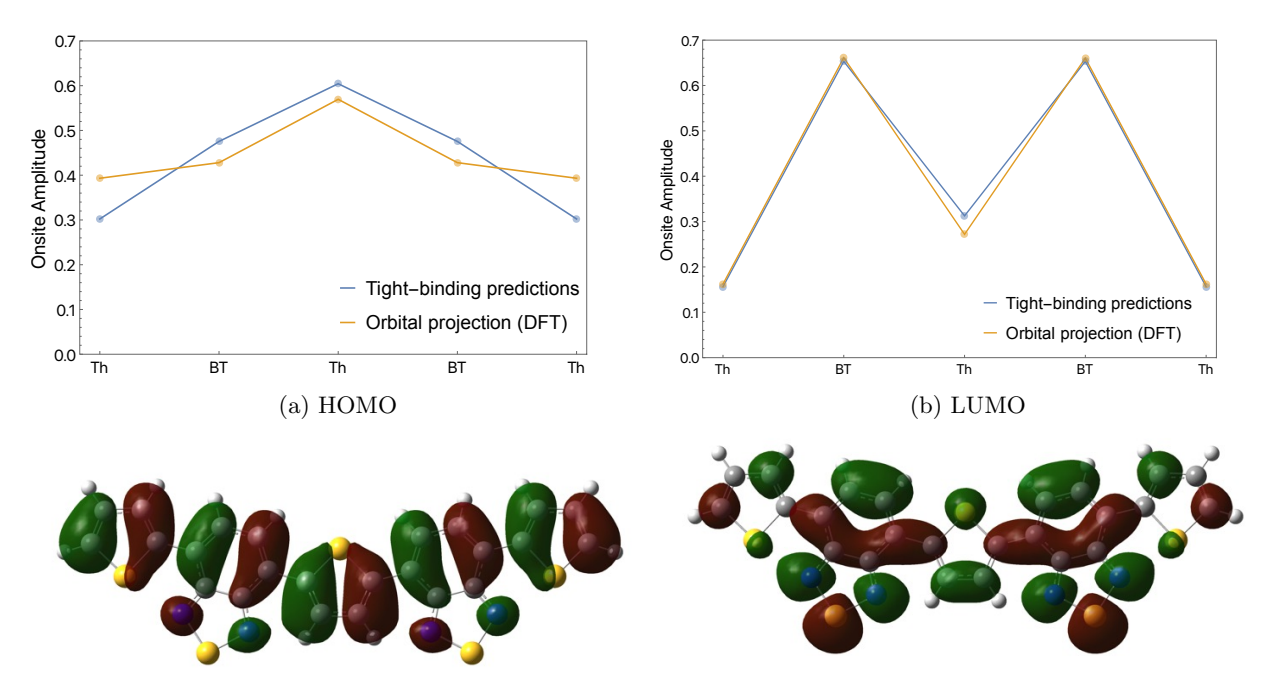


Figure 10: Onsite amplitudes of HOMO (a) and LUMO (b) wavefunction obtained using orbital projection of DFT results (orange), compared to tight-binding predictions (blue) with fitted parameters for thiophene - benzothiadiazole pentamer. At bottom are the corresponding orbital images from Gaussian. Iso-value of 0.01 is used for orbital surfaces.

energies of thiophene and BT moieties.

The analytical solution to the tight-binding Hamiltonian for alternating co-oligomers is given in the appendix.

The eigenvector  $\psi_k$  takes the form

$$\psi_k \propto f^{(-1)^k} \sin\left(\frac{\pi k}{n+1}\right) \tag{8}$$

in which the front factor  $f^{(-1)^k}$  alternates between 1/f for odd sites and f for even sites corresponding to two different comonomers, and f depends on the mismatch between the two comonomers. The orbital images in Fig. 10 display DFT HOMO and LUMO of a thiophene-BT pentamer, which consists of a combination of the monomer HOMO and LUMO orbitals. Such agreement is also observed for the other two alternating co-oligomers.

Table 2 reports the fitted values of the hopping matrix elements for all three types of co-oligomers. The symmetry of the local orbitals dictates the sign of the hopping matrix elements. This result from the definition of the hopping matrix elements as an integral of the product of a symmetric potential and the two interacting orbitals. For thiophene, phenylene and BT, the HOMO is antisymmetric under reflection on the plane normal to the ring, whereas the LUMO is symmetric (see Fig 4). The symmetric monomer LUMOs lead to a positive value for  $t_L$ , whereas a negative value of  $t_H$  is a result of the antisymmetric monomer HOMOs.

Table 2: Hopping matrix elements (in eV) for thiophene-phenyl (ThBz), thiophene-benzothiadiazole (ThBT), and rhodanine-benzothiadiazole (RhBT) oligomers.

Comonomers	$t_H$	$t_L$
Th-Bz	-0.72	0.82
Th-BT	-0.60	0.65
Rh-BT	-0.15	0.60

### Dihedral dependence of hopping matrix element

Dihedral disorder affects conjugation along an oligomer, which has a strong effect on optoelectronic properties and localization of charge carriers. In a tight-binding model, distortions of the inter-ring dihedral angle breaks the overall molecule planarity. This distortion is captured by making the hopping matrix element dependent on this dihedral angle. The hopping matrix element  $t_{\theta}$  between two monomers vary as the cosine of the dihedral angle  $\theta$  between the co-monomers.

$$t_{\theta} = t \cos(\theta) \tag{9}$$

where t is the hopping matrix element between two sites for a planar configuration, i.e., when  $\theta = 0^{\circ}$ .

Fig. 11 compares the frontier orbital energies for a thiophene hexamer predicted by our tight-binding model to DFT results as a function of the central dihedral angle  $\theta_3$ . The hopping matrix element for central

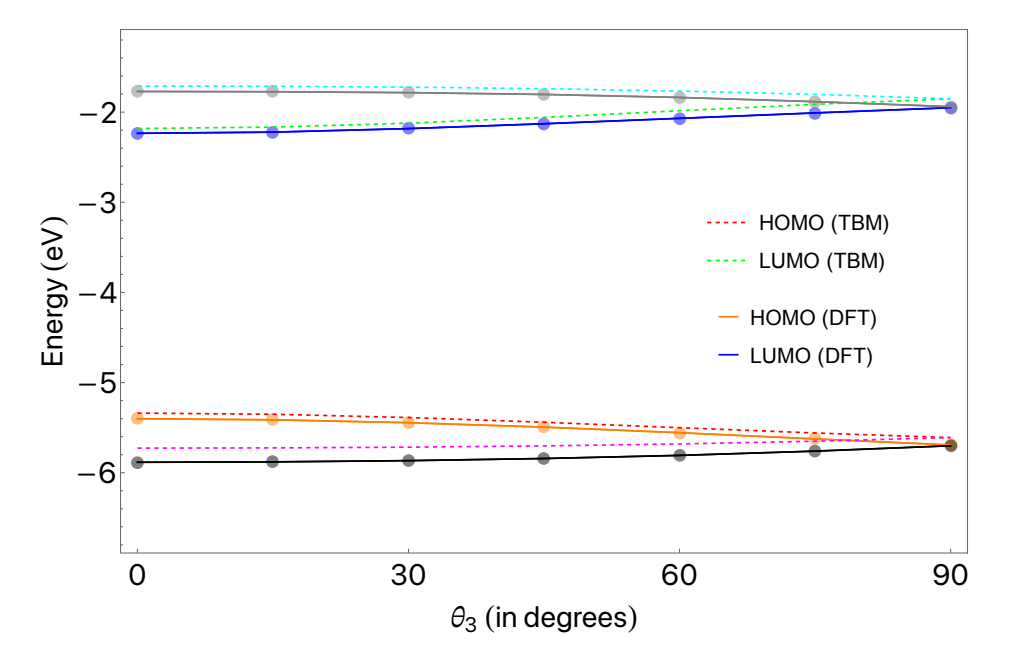


Figure 11: HOMO (orange points) and LUMO (blue points) energy from DFT calculations by varying dihedral angle ( $\theta_3$ ) about the central bond of a thiophene hexamer, compared to tight-binding predictions (red and green dashed curves) with cosine hopping matrix element,  $t_3 = \cos(\theta_3)$ . HOMO-1 (black points, pink dashed curve) and LUMO+1 (gray points, cyan dashed curve) energy using DFT calculations and predicted using tight-binding model.

bond  $t_3 = t_{Th} \cos(\theta_3)$  is used to describe the tight-binding Hamiltonian for thiophene hexamer, while the other off-diagonal terms are set equal to  $t_{Th}$  as appropriate for a planar configuration. Fig. 11 shows that the tight-binding model accurately predicts the HOMO and LUMO energies for varying dihedral angle  $\theta_3$ , compared to DFT results.

Fig. 12 shows the corresponding DFT molecular orbitals. Fig. 13 compares the LUMO onsite amplitudes of the tight-binding prediction with those obtained using orbital projection of DFT molecular orbitals. For  $\theta_3 = 90^{\circ}$ , the hopping matrix element  $t_3$  vanishes as the molecular fragment on either side rotates completely out of plane, which breaks the  $\pi - \pi$  conjugation (Fig. 12c). The charge carriers localize on the trimer fragments (red dashed curves in Fig. 13), and degenerate pairs of HOMO and HOMO-1, and LUMO and LUMO+1 are obtained which can be observed in Fig. 11 for  $\theta = 90^{\circ}$ . Thus, the tight-binding model also predicts the changes in shape of frontier orbitals when the dihedral is rotated, in good agreement with DFT results.

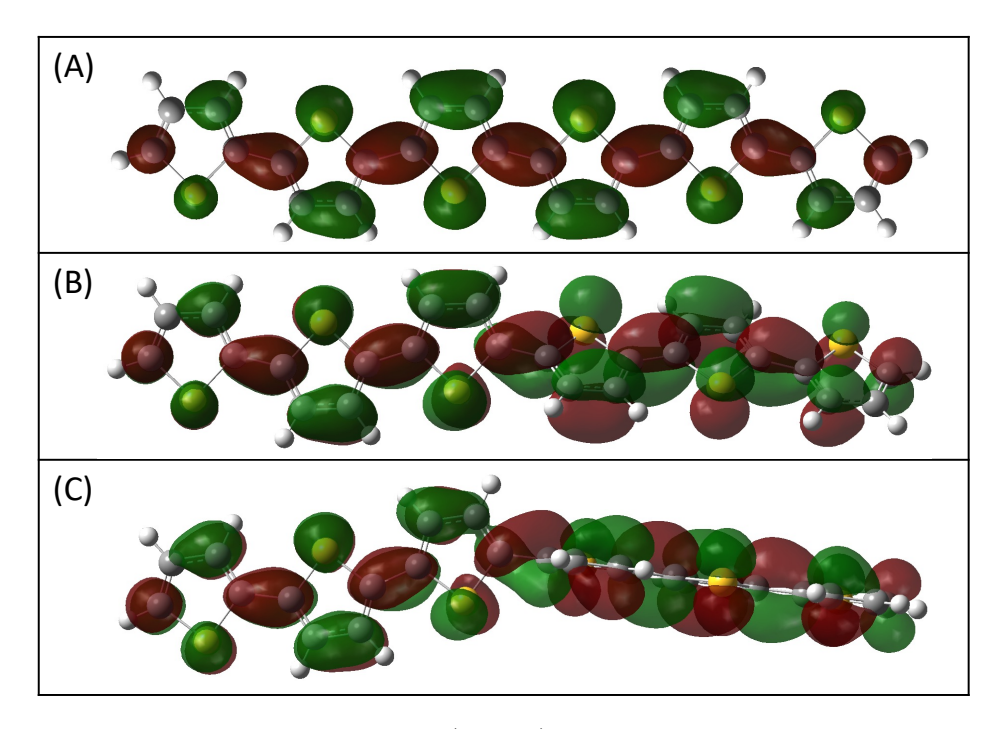


Figure 12: Lowest unoccupied molecular orbital (LUMO) wavefunctions from DFT calculations by varying dihedral angle ( $\theta_3$ ) about the central bond of a thiophene hexamer for (A)  $\theta_3 = 0^0$ , (B)  $\theta_3 = 45^0$  and (C)  $\theta_3 = 90^0$ . An iso-surface of 0.01 is used to plot the wavefunctions using B3LYP/6-311g(d) in Gaussian.

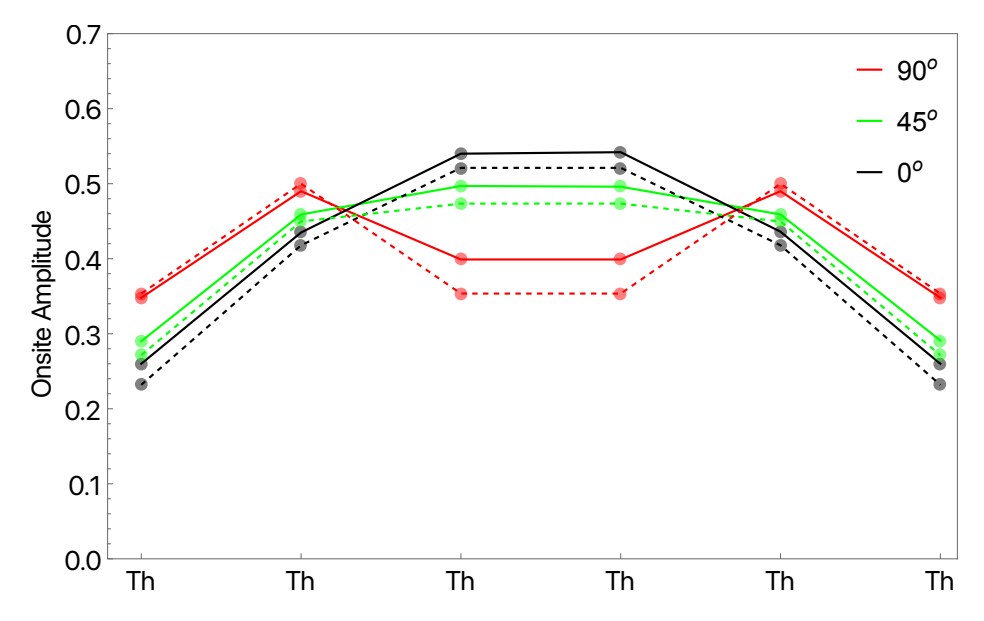


Figure 13: Onsite amplitudes of thiophene hexamer LUMO wavefunction obtained using orbital projection of DFT results (solid curve), compared to tight-binding predictions (dashed) for  $\theta_3$  of  $0^o$  (black),  $45^o$  (green) and  $90^o$  (red).

# 4 Tight-binding predictions for IDTBR

Tables 1 and 2 list the tight-binding parameters fitted for homo-oligomers and alternating co-oligomers made from constituent monomers of IDTBR. From these values, we predict the characteristics of charge carriers

on IDTBR with no further adjustment.

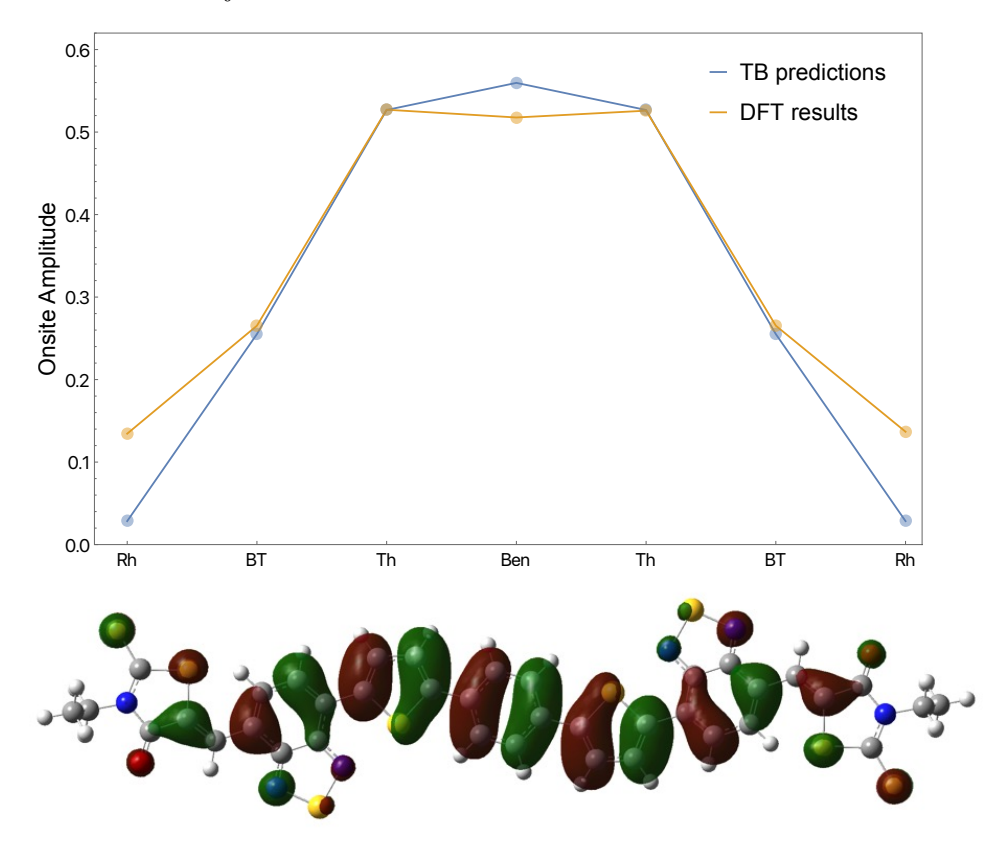


Figure 14: Onsite amplitudes of HOMO wavefunction obtained using orbital projection of DFT results (orange), compared to tight-binding predictions (blue) with fitted parameters for IDTBR. At bottom is the orbital image from Gaussian. Iso-value of 0.01 is used for orbital surfaces.

Table 3 presents the tight-binding predicted HOMO and LUMO energies for IDTBR, both of which compare well with DFT calculations. Figures 14 and 15 display the predicted wavefunction, which compare reasonably well to the onsite amplitudes obtained using orbital projection method from DFT results.

Table 3: Frontier orbital energies (in eV) of IDTBR from tight-binding and DFT calculations.

Method	TBM	DFT
HOMO	-5.54	-5.74
LUMO	-3.57	-3.65

The IDTBR HOMO is mainly concentrated on the electron-rich core, whereas the LUMO has larger amplitudes on the more electronegative, BT and rhodanine, end groups. The tight-binding model represents the IDTBR HOMO and LUMO, both qualitatively and quantitatively, well, except the onsite amplitude of rhodanine. The model underestimates the amplitude on rhodanine for the IDTBR HOMO, while it overestimates the amplitude of rhodanine for the LUMO.

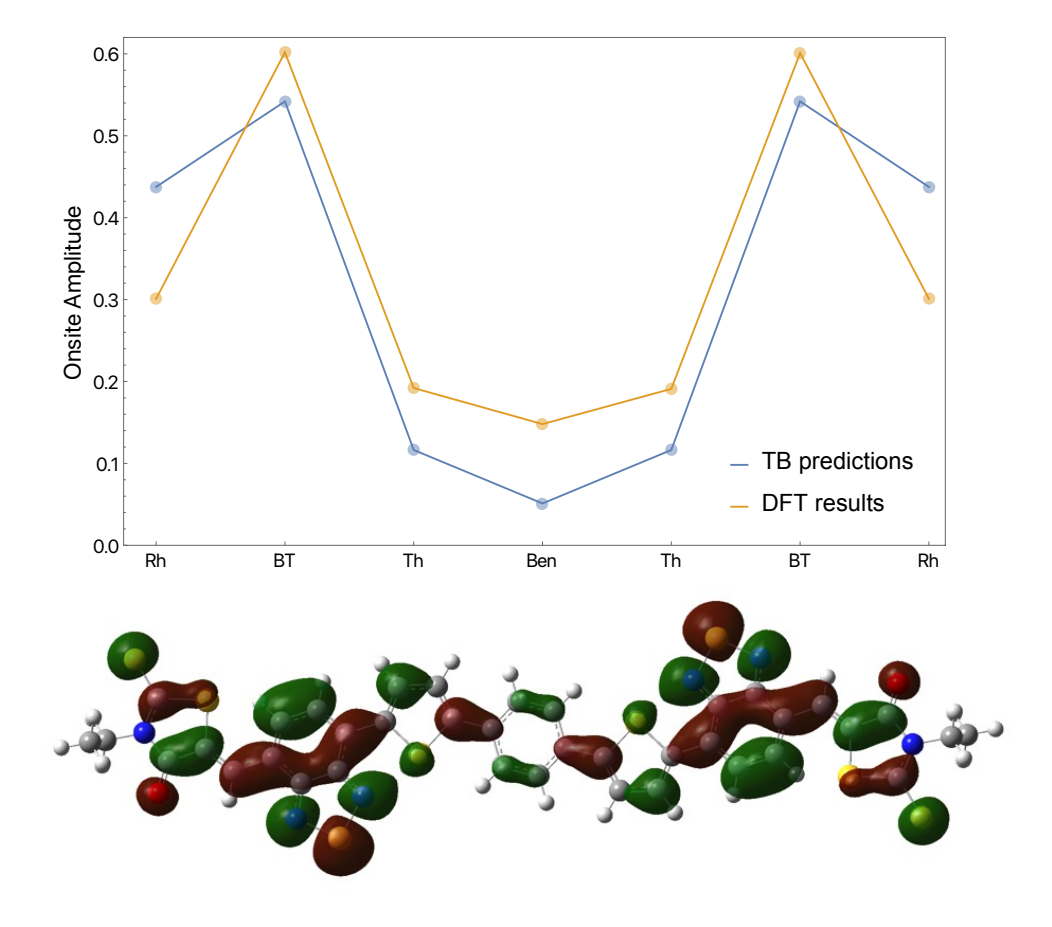


Figure 15: Onsite amplitudes of LUMO wavefunction obtained using orbital projection of DFT results (orange), compared to tight-binding predictions (blue) with fitted parameters for IDTBR. At bottom is the orbital image from Gaussian. Iso-value of 0.01 is used for orbital surfaces.

Because the IDTBR LUMO mostly sits on the end groups, the disagreement between predicted and DFT onsite amplitude on rhodanine is more pronounced. For rhodanine, it appears that non-LUMO states may also participate to form the IDTBR LUMO. Overall, the tight-binding model performs well, predicting both the energy levels and wavefunctions of the IDTBR HOMO and LUMO.

The convenient feature of tight-binding models is the ease with which the model can be modified to represent a molecule of similar architecture. We demonstrate this by constructing a tight-binding model for 4F-IDTBR, in which both benzothiodiazole moieties are doubly fluorinated.

Fluorination of benzothiadiazole has been claimed to increase the propensity for  $\pi - \pi$  stacking, which promotes crystallization and improves device performance. [37] Gomez et al. have found experimentally more  $\pi$ -stacking in fluorinated donor-acceptor co-polymers. [38] The attractive interactions between the electron-rich donor and fluorinated electron-deficient acceptor units have been argued to induce very tightly stacking

crystallites, which reduce the energetic barrier for charge hopping. Substitution of only a few fluorines on a large molecule does not significantly affect miscibility with non-fluorinated conjugated polymers. [39] In any case, the core and side chains of acceptors can be perturbed to tune the propensity for crystallization and miscibility with donor polymers.

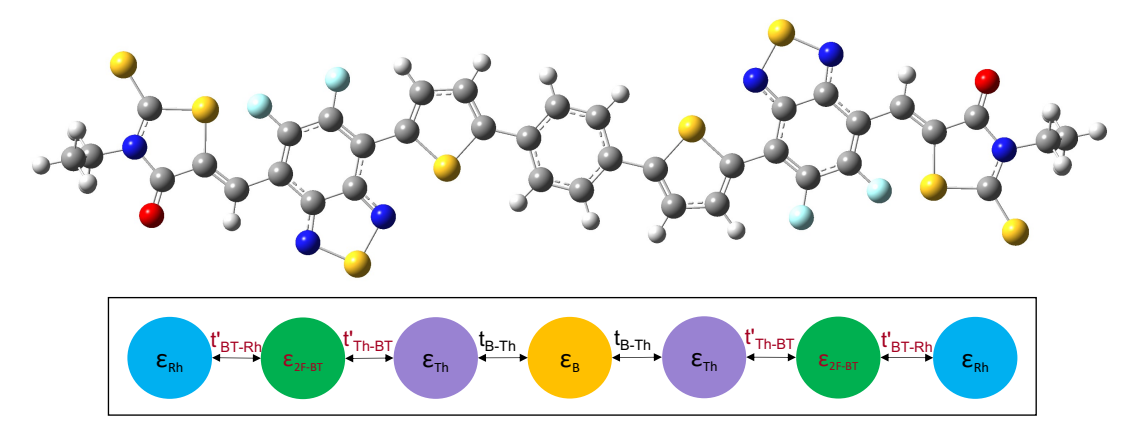


Figure 16: Fluorinated IDTBR (4F-IDTBR) and its modified tight-binding model. Fluorinated benzothia-diazole (2F-BT) moiety is represented as a green circle. Modified TB parameters are labeled in dark red.

We can use a tight-binding model to computationally screen the electronic properties, including frontier orbital energies and wavefunctions, of modified acceptor molecules like 4F-IDTBR. Fig. 16 displays the tight-binding model for 4F-IDTBR, which has three modified parameters: the onsite energy  $(\epsilon_{2F-BT})$  of 5,6-Difluoro-2,1,3-benzothiadiazole (2F-BT), and the hopping matrix elements  $(t'_{Th-BT}, t'_{BT-Rh})$  between 2F-BT and the adjacent, thiophene and rhodanine, moieties.

The modified parameters are estimated by fitting frontier orbital energies of varying length of homo-oligomers and alternating co-oligomers containing 2F-BT. The rest of the tight-binding parameters are taken from the IDTBR model without any modification. Fig. 17 shows the HOMO and LUMO energies fitted using a tight-binding model to the DFT calculations on 2F-BT oligomers of varying length, from which we fit the onsite energy  $\epsilon_{2F-BT}$ .

We estimate  $t'_{Th-BT}$  and  $t'_{BT-Rh}$  using thiophene-(2F)BT alternating co-oligomers and a rhodanine-(2F)BT dimer, respectively. Fig. 18 compares HOMO and LUMO energies versus co-oligomer length from DFT and tight-binding calculations for thiophene-(2F)BT alternating co-oligomers. Table 4 lists the values of all the modified parameters used to define the tight-binding model of 4F-IDTBR.

Having modified these three tight-binding parameters, we can predict frontier orbital energies and wavefunctions for 4F-IDTBR. Table 5 compares the frontier orbital energies for 4F-IDTBR and IDTBR from the

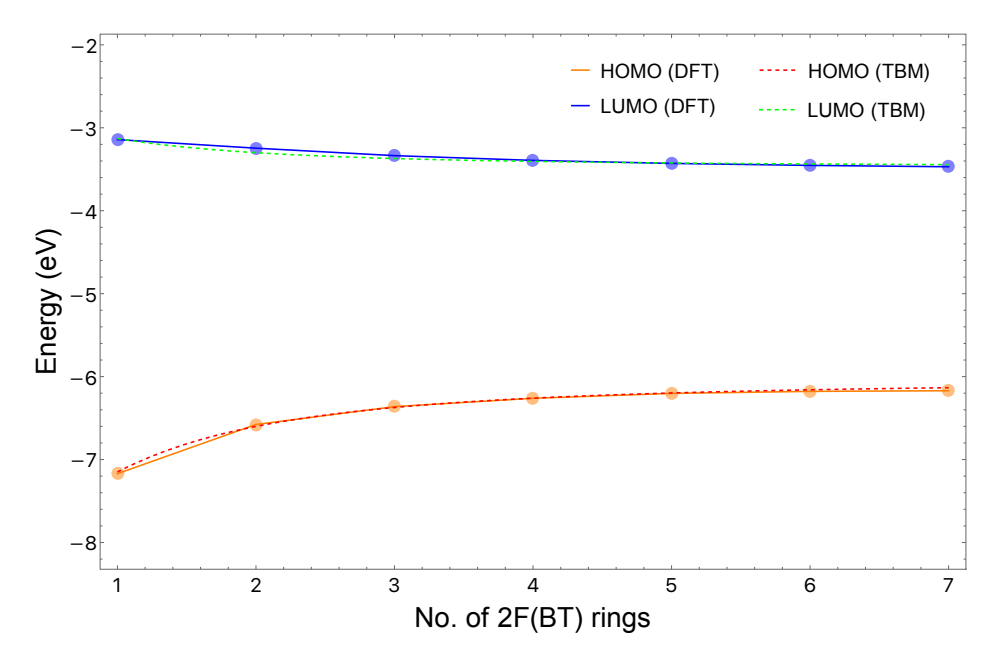


Figure 17: HOMO (orange points) and LUMO (blue points) energy (in eV) from DFT calculations on (2F)BT homo-oligomers, compared to tight-binding predictions with fitted parameters (red and green dashed curves).

Table 4: Modified parameters in the tight-binding model of 4F-IDTBR (marked red in Fig. 16) compared to parameters used for IDTBR.

4F-IDTBR	НОМО	LUMO	IDTBR	НОМО	LUMO
$\epsilon_{2F-BT}$	-7.15	-3.13	$\epsilon_{BT}$	-6.80	-2.90
$t'_{Th-BT}$	-0.55	0.65	$t_{Th-BT}$	-0.60	0.65
$t'_{BT-Rh}$	-0.55	0.95	$t_{BT-Rh}$	-0.15	0.60

tight-binding model and DFT calculations. The frontier orbital energies of both IDTBR and 4F-IDTBR are predicted quite accurately; compared to DFT results, tight-binding HOMO energies are off by 0.2-0.3 eV, and LUMO energies are within 0.1 eV.

Table 5: Energy (in eV) for frontier orbitals of 4F-IDTBR using tight-binding method and DFT calculations compared to IDTBR.

Energy (eV)	TBM	DFT
4F-IDTBR HOMO	-5.58	-5.89
4F-IDTBR LUMO	-4.04	-3.94
IDTBR HOMO	-5.54	-5.74
IDTBR LUMO	-3.57	-3.65

Fig. 19 and 20 compare HOMO and LUMO wavefunctions of 4F-IDTBR predicted using the tight-binding model with DFT results. These predictions reproduce the onsite amplitudes at the core of the molecule reasonably well but perform less well for the rhodanine end groups. The discrepancies in predicted wavefunction on rhodanine may reflect the contribution of non-frontier orbitals of rhodanine to the molecular frontier orbitals on IDTBR and 4F-IDTBR. But overall, the tight-binding model with custom tuned param-

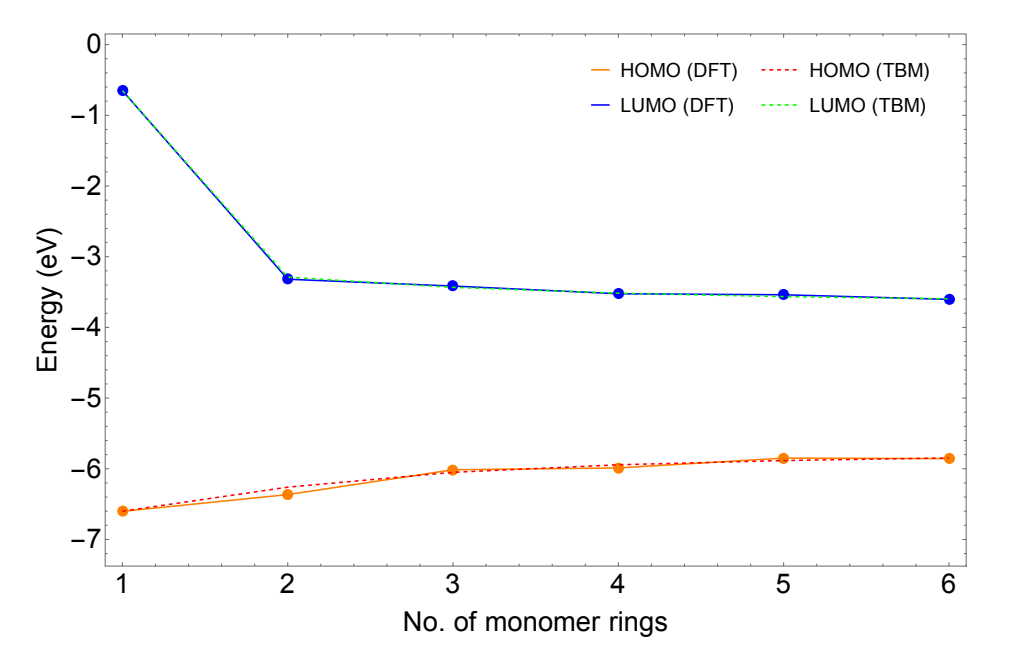


Figure 18: HOMO (orange points) and LUMO (blue points) energy (in eV) from DFT calculations on thiophene-(2F)BT co-oligomers, compared to tight-binding predictions with fitted parameters (red and green dashed curves).

eters predict the LUMO wavefunction reasonably well compared to DFT results; and the LUMO structure is most important for future work in describing polarons and charge-transfer excitons on these promising acceptors.

Further, the tight-binding model accounts for the effect of dihedral disorder on frontier orbitals, because hopping matrix elements depend on inter-ring dihedral angles between constituent rings. For IDTBR, we vary one of the thiophene-BT dihedral angles to compare the HOMO and LUMO energies predicted by the tight-binding model to DFT results. Fig. 21 shows that the HOMO and LUMO energy levels do not change much as  $\theta$  varies, in both DFT and tight-binding results. However, the wavefunction shape changes substantially as we rotate the dihedral. For the LUMO, Fig. 22(a) shows that the BT and rhodanine onsite amplitudes on the right end of IDTBR gradually decrease, in both DFT and tight-binding results.

Fig. 23 compares the HOMO and LUMO wavefunctions of IDTBR predicted using the tight-binding model to DFT for  $\theta=0^o$  and  $90^o$ . DFT agrees with the tight-binding predictions except for the quantitative discrepancies on rhodanine at the ends already remarked upon. In both tight-binding and DFT results, a dihedral angle of  $90^o$  limits conjugation beyond the right-hand thiophene, which shifts the LUMO entirely to the other end of IDTBR. Overall, the tight-binding model performs well as we introduce dihedral distortions, predicting both the variations in energy levels and wavefunctions of the IDTBR frontier orbitals.

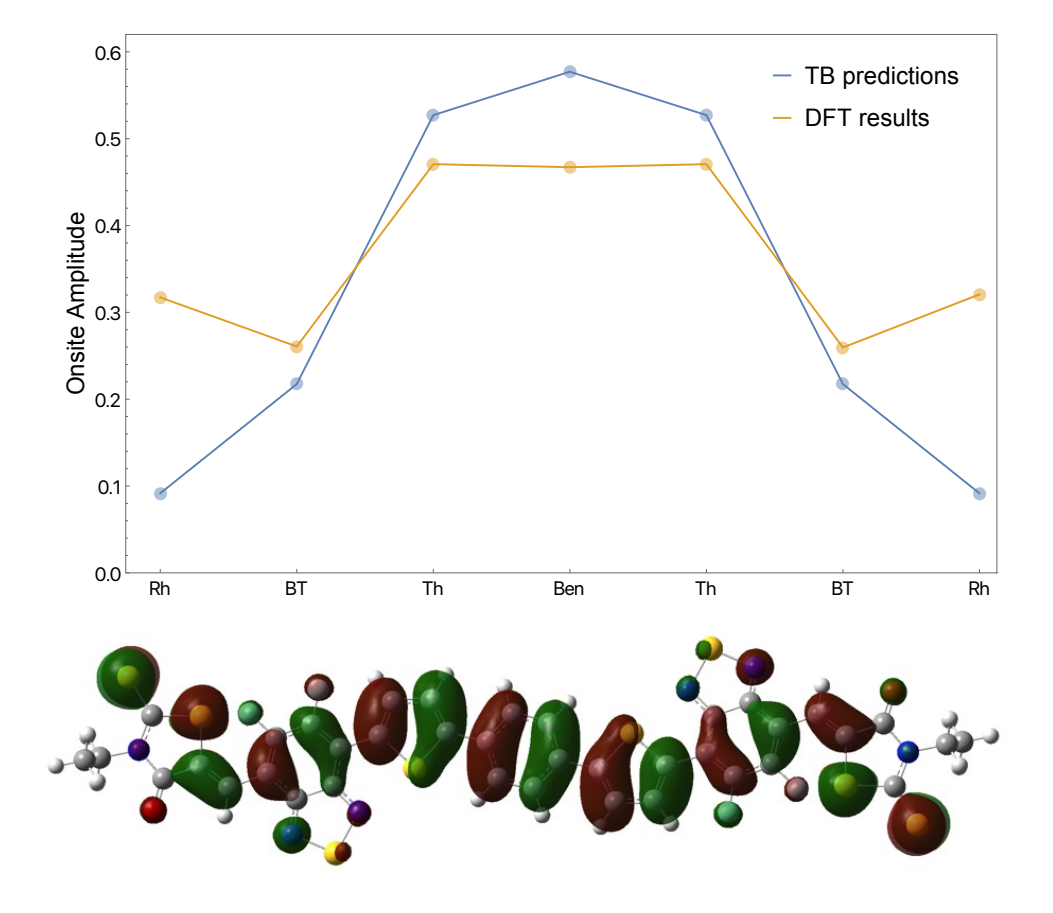


Figure 19: Onsite amplitudes of HOMO wavefunction obtained using orbital projection of DFT results (orange), compared to tight-binding predictions (blue) with fitted parameters for 4F-IDTBR. At the bottom is the orbital image from Gaussian. An iso-value of 0.01 is used for orbital surfaces.

# 5 Conclusion

Frontier orbitals on conjugated oligomers predominately consist of linear combination of frontier orbitals on the constituent monomers. This observation motivates the construction of tight-binding models, which achieve computational efficiency by drastically reducing the number of degrees of freedom, while still representing the important frontier orbitals. We extend a coarse-grained approach based on the tight binding approximation to model frontier orbitals on oligomers and non-fullerene acceptors, which enables efficient calculations of optoelectronic properties for conjugated small molecules used in organic solar cells.

Aromatic ring constituents of the conjugated molecules are good building blocks for tight-binding model because they are rigid, so that their local electronic properties are nearly fixed as the molecule changes conformation. Conformational disorder is dominated by the flexible dihedrals between the rings, and charge delocalization across the conjugated molecule depends on the hopping terms which vary as cosine of dihedral angles.

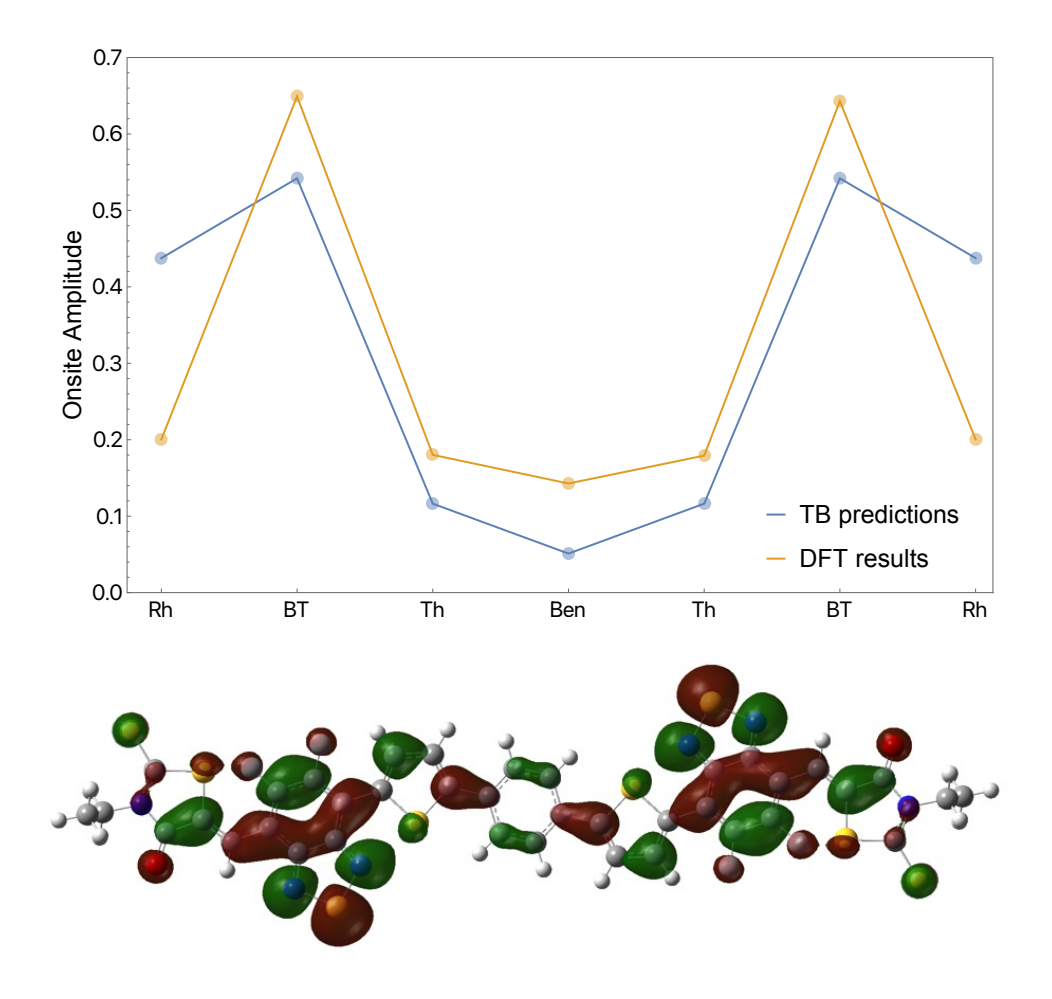


Figure 20: Onsite amplitudes of LUMO wavefunction obtained using orbital projection of DFT results (orange), compared to tight-binding predictions (blue) with fitted parameters for 4F-IDTBR. At the bottom is the orbital image from Gaussian. An iso-value of 0.01 is used for orbital surfaces.

We demonstrate our approach on a variety of homo-oligomers and alternating co-oligomers constructed from commonly studied conjugated monomers including thiophene, phenylene, benzothiadiazole, and rhodanine. Finally, we show the tight-binding approach describes frontier energies and orbitals on hetero-oligomers including IDTBR and 4F-IDTBR, which are non-fullerene acceptors designed to give high-performing organic photovoltaics with polymeric donor materials.

We present a straightforward scheme for fitting tight-binding model parameters, which are the onsite energies and hopping matrix elements, by comparison to DFT HOMO and LUMO energies for series of homo-oligomers and alternating co-oligomers of varying length. These locally determined parameters when used as building blocks are transferable from homo-oligomers and alternate co-oligomers without changing, for different conformations and different molecular architectures including hetero-oligomers.

Tight-binding model predictions for IDTBR HOMO and LUMO energies and wavefunctions are consistent

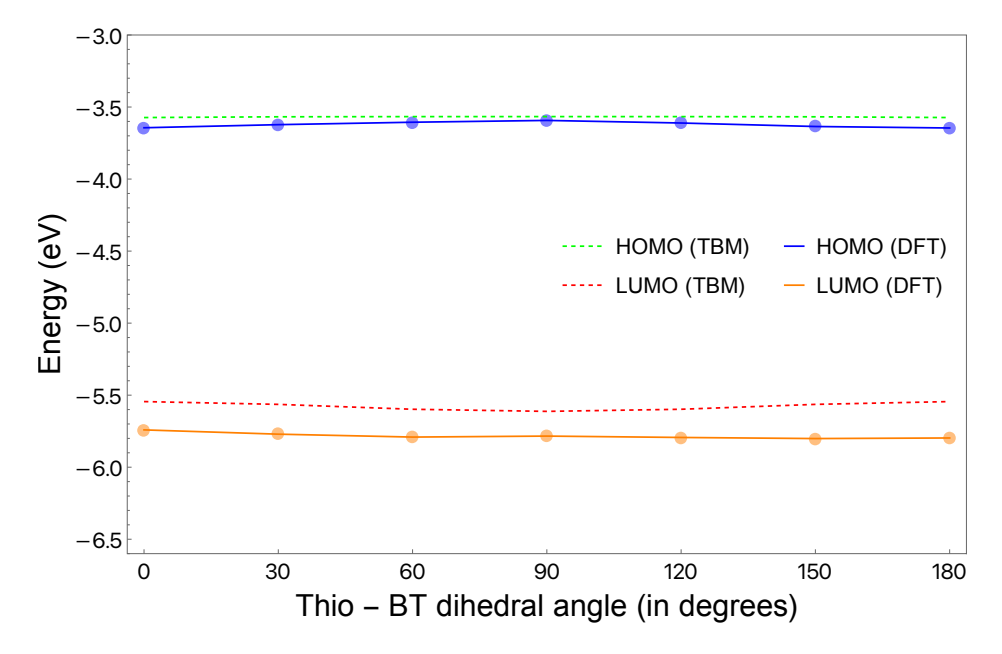


Figure 21: HOMO (orange points) and LUMO (blue points) energy from DFT calculations by varying thiophene - BT dihedral angle ( $\theta$ ) of IDTBR, compared to tight-binding predictions (red and green dashed curves) with cosine hopping matrix element,  $t_{Th-BT} = \cos(\theta)$ .

with DFT results. In this work, we consider DFT calculations (here performed with the hybrid B3LYP functional and 6-311g(d) basis set) as standards for the electronic structure of molecules, to explore the potential for tight binding models to efficiently reproduce more expensive DFT calculations. Evidently, the accuracy of tight binding models parameterized using DFT would be subject to the same limitations faced by DFT calculations; likewise, improvement in DFT accuracy could be immediately transferred to improve tight-binding parameters.

Calculation of frontier orbitals using our approach is efficient, both in terms of computation time and required number of parameters. There are of course limitations to our approach. 1) The tight-binding model is not good for states far from frontier orbitals. At best, for extended molecules, one may expect to calculate low-lying non-frontier molecular orbitals in terms of the same set of site frontier orbitals, but eventually, states away from the oligomer frontier orbitals will mix in contributions from higher-lying orbitals on the individual sites that were neglected in the tight-binding model. 2) The constituent sites should be correctly chosen; for efficiency, they should be as large as possible, but at the same time conformationally rigid and tightly coupled electronically, and small enough such that their closely spaced orbital energies do not require more than a single frontier orbital to be retained. These considerations motivate us to use single aromatic rings as sites. The resulting approach is well designed for conjugated molecules consisting of ringlike moieties bonded together, which covers a broad class of organic semiconductors.

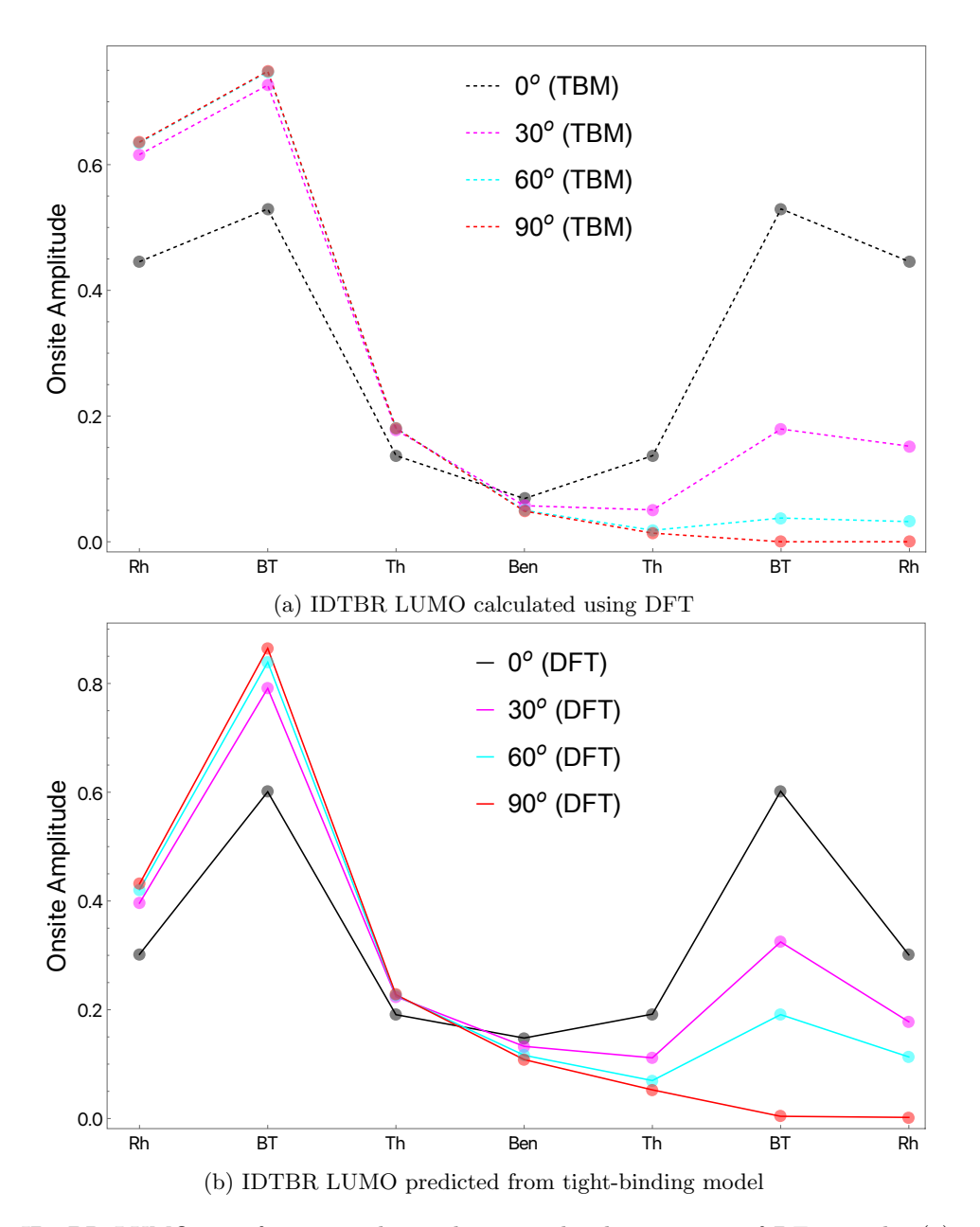


Figure 22: IDTBR LUMO wavefunctions obtained using orbital projection of DFT results (a) and tight-binding model (b) for thiophene - BT dihedral angle of  $0^{o}$  (black),  $30^{o}$  (cyan),  $60^{o}$  (magenta) and  $90^{o}$  (red).

Our model as presented only considers isolated molecules, and we acknowledge that it is important to consider interactions with the surrounding medium [40], including possible interchain coupling, perturbation of onsite energies, and/or impacts on chain structure, to accurately predict bulk material properties. [21]

The tight-binding model developed here can be extended to predict optoelectronic properties of extended conjugated systems, including optical gaps, excitons at donor-acceptor interfaces, and structure and transport of excitons and polarons in dielectric media. Excitons can be described as interacting electron-hole pairs,

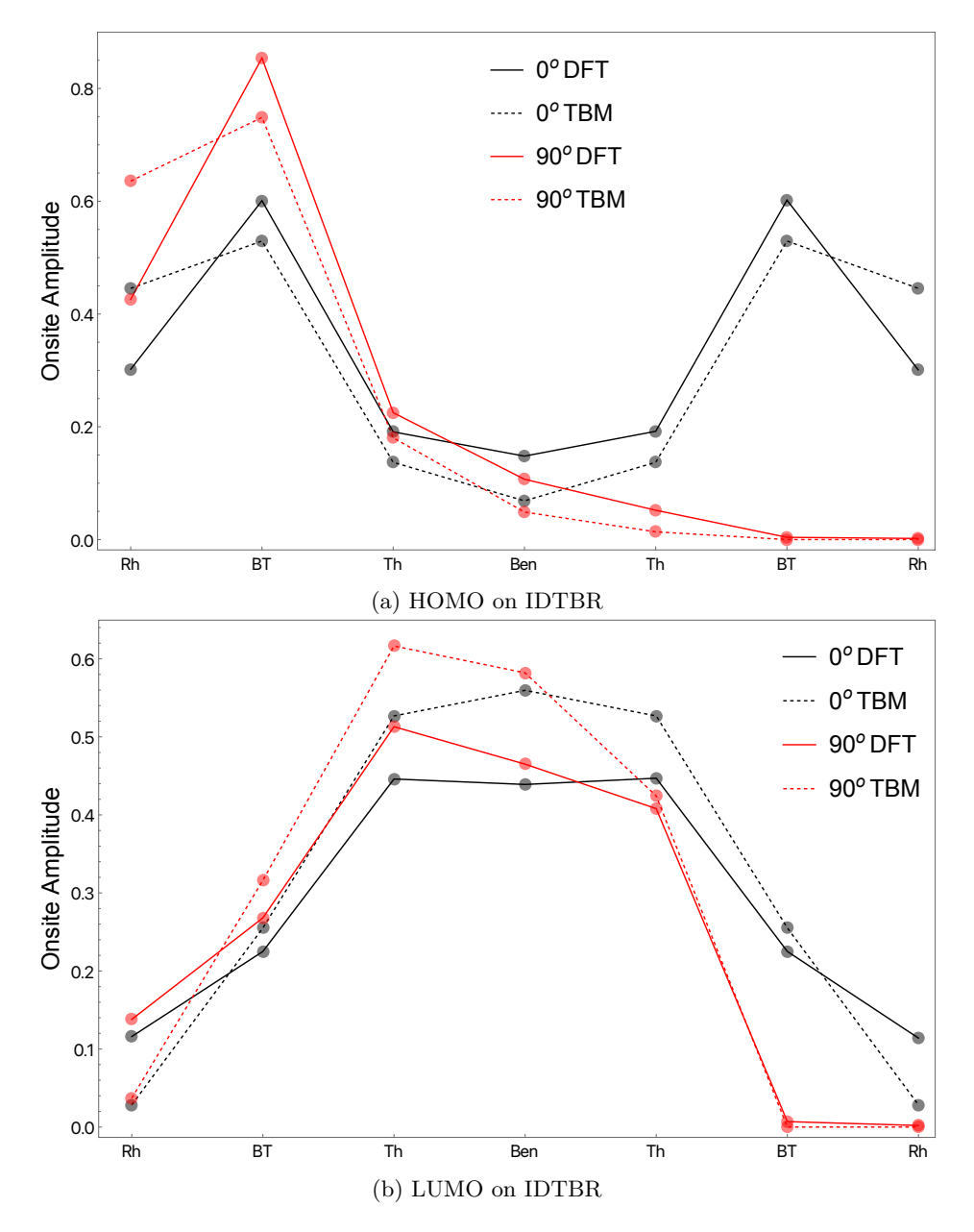


Figure 23: IDTBR frontier orbital wavefunctions obtained using orbital projection of DFT results (solid curve), compared to tight-binding predictions (dashed) for thiophene - BT dihedral angle of  $0^o$  (black) and  $90^o$  (red).

accounting for Coulomb interactions with direct and exchange terms. The tight-binding model offers the advantage of calculating direct and exchange Coulomb integrals explicitly. By minimizing the total energy over the shape of the electron and hole, the exciton can be accurately determined, accounting for competition between the electron-hole Coulomb interaction and the kinetic energy of the electron and hole. Polarons can be described by introducing a charge on the molecule that interacts with the surrounding dielectric media, represented as a continuum. The shape of the polaron on the molecule is obtained by minimizing the sum

of the interaction energy with the surrounding media and the kinetic energy of the charge. [21] The tightbinding approach makes such excited state predictions computationally feasible, particularly when dealing with large system sizes, conformational disorder, and environmental irregularities that pose challenges for DFT calculations. We will report results exploiting this approach in forthcoming publications.

# 6 Conflicts of interest

There are no conflicts of interest to declare.

# 7 Acknowledgements

The authors acknowledge funding provided by the Office of Naval Research (ONR) (grant number N00014-19-1-2453), and Institute for Computational and Data Sciences (ICDS) at Penn State for providing high-performing computation resources through Roar Supercomputer.

# A Analytical solution for tight-binding model

Here, we present analytical solutions for the wavefunctions and energies of both homo-oligomers and alternating co-oligomers described by tight-binding models.

### A.1 Homo-oligomers

The tight-binding model can be used to compute the HOMO and LUMO of homo-oligomers. In matrix form, the tight-binding Hamiltonian is

$$H = \begin{bmatrix} \epsilon & -t \\ -t & \epsilon & -t \\ & -t & \epsilon & -t \\ & & \ddots & \\ & & & -t & \epsilon \end{bmatrix}$$

$$(10)$$

If the matrix extended indefinitely in both directions (as for a one-dimensional infinite chain), then by inspection plane waves of the form  $\psi_j = e^{ikj}$  are eigenfunctions. On inserting such a form into  $H\psi = E\psi$ ,

the jth equation takes the form

$$-te^{ik(j-1)} + \epsilon e^{ikj} - te^{ik(j+1)} = Ee^{ikj}$$

$$\tag{11}$$

The above equation is satisfied for an energy E given by

$$E(k) = \epsilon - 2t\cos k \tag{12}$$

for any value of k. Note that we can take k either positive or negative (corresponding to left-going and right-going waves once time-dependence is restored), both of which have the same energy E(k).

For a long chain, the difference in energies for the maximally bonding and antibonding states, corresponding to  $k = \pi/(n+1)$  and  $k = n\pi/(n+1)$ , leads to a HOMO-LUMO gap of

$$\Delta E = 2t \left(\cos(\pi/(n+1)) - \cos(\pi n/(n+1))\right)$$

$$\approx 4t \left(1 - \frac{\pi^2}{2(n+1)^2}\right)$$
(13)

Thus the difference in the lowest and highest eigenvalues approaches the expected long-chain limit of 4t (i.e., the full bandwidth for a cosine band of a 1d chain), with linear corrections of order  $1/n^2$ .

For a finite oligomer of n sites, we need the wavefunction to vanish on both sites just beyond the end of the actual oligomer, i.e., for j = 0 and j = n + 1. We can satisfy the boundary condition at j = 0 for any k, by combining the left- and right-going waves as  $e^{ikj} - e^{-ikj}$ , or equivalently by taking

$$\psi_k(j) \propto \sin(kj) \tag{14}$$

with normalization to be set later.

Now we must choose k to satisfy the boundary condition that  $\psi$  vanishes at the other end, j = n + 1. Hence we have

$$k = \frac{m\pi}{n+1}$$
 ,  $m = 1, 2, 3, \dots$  (15)

corresponding to sine functions with  $0, 1, 2, \ldots$  nodes.

To normalize the wavefunction  $\psi_k(j) \propto \sin(kj)$ , we must compute the sum of its square amplitudes,

$$S = \sum_{j=1}^{n} \sin^2(kj) \tag{16}$$

We can extend the sum to j = n + 1 since that term vanishes. Now insert the definition of sin in terms of complex exponentials, to obtain

$$S = (1/4) \sum_{j=1}^{n+1} \left( 2 - e^{2ikj} - e^{-2ikj} \right)$$
 (17)

For any k of the form  $k = m\pi/(n+1)$ , the points swept out by the sums over the complex exponentials are equally spaced around the unit circle. So by symmetry in the complex plane, the second and third sums vanish; hence S = (n+1)/2, and the normalized wavefunction is

$$\psi_k(j) = \sqrt{2/(n+1)}\sin(kj) \tag{18}$$

In summary, the lowest eigenvector of the Hamiltonian matrix is

$$\psi_1(j) = \sqrt{2/(n+1)}\sin(\pi j/(n+1)) \tag{19}$$

in which j runs over the site indices  $1, \ldots n$ , vanishing at the "phantom sites" just beyond the ends of the oligomer, at j = 0 and j = n + 1. The highest eigenvector is the same sine function, but with a sign change between every pair of adjacent sites:

$$\psi_n(j) = (-1)^j \sqrt{2/(n+1)} \sin(\pi j/(n+1)) \tag{20}$$

This analytical expression for the wavefunction (red curve) exactly matches eigenvectors numerically computed from the Hamiltonian matrix (blue dots), as can be seen in Fig. 24.

## A.2 Alternating co-oligomers

Consider a tight-binding Hamiltonian for an alternating copolymer, in which the onsite energy difference between odd and even sites equals  $2\epsilon$ .

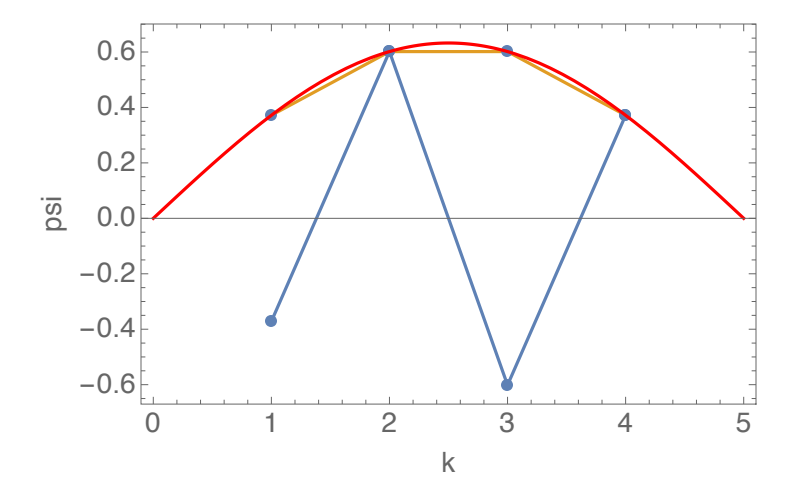


Figure 24: Lowest and highest wavefunctions for n = 4, computed numerically versus analytically (Eqs. 19 and 20).

The Hamiltonian takes the form

$$H = \begin{bmatrix} 2 + d\epsilon & -1 \\ -1 & 2 - d\epsilon & -1 \\ & -1 & 2 + d\epsilon & -1 \\ & & & \dots \\ & & & -1 & 2 + \epsilon \end{bmatrix}$$
(21)

Here for simplicity of presentation we measure energies in units of the hopping matrix element t between sites, and set the zero of energy so that a uniform state  $\{1, 1, ... 1\}$  has zero energy. We undo this scaling and shifting later, as shown in the end.

By numerical experiments with this Hamiltonian, it appears the lowest energy eigenfunction takes the form of a modulated sinusoidal envelope, in which the amplitude on site k is proportional to  $\sin(\pi k/(n+1))$ , times a factor depending on whether the site index k is even or odd. In the limit  $d\epsilon \to 0$ , there is no modulation between even and odd sites, and we recover the homopolymer behavior computed in the previous section.

We therefore guess an eigenfunction of this form,

$$\psi_k \propto f^{(-1)^k} \sin\left(\frac{\pi k}{n+1}\right) \tag{22}$$

in which the front factor  $f^{(-1)^k}$  is designed to alternate between 1/f for odd sites and f for even sites.

With this guess, we can write equations corresponding to odd and even rows of the eigenfunction equation  $H\psi = E\psi$ . For convenience, we write the sine factor in  $\psi$  as the imaginary part of  $e^{i\pi k/(n+1)}$ . Then for odd rows we have

$$-f\left(e^{i\pi/(n+1)} + e^{-i\pi/(n+1)}\right) + (2+d\epsilon)(1/f) = E(1/f)$$
(23)

and for even rows,

$$-(1/f)\left(e^{i\pi/(n+1)} + e^{-i\pi/(n+1)}\right) + (2+d\epsilon)f = Ef$$
(24)

The top and bottom rows in the matrix have the same equation, because we can regard the eigenfunction as having sites k = 0 and k = n + 1, both with zero amplitude.

These are two equations with two unknowns E and f. We can eliminate E to obtain

$$f^{2} - (1/f)^{2} = \frac{d\epsilon}{\cos(\pi/(n+1))}$$
 (25)

This is a quadratic equation for the even/odd ratio  $f^2$ , with solution

$$f^2 = \frac{Q + \sqrt{Q^2 + 4}}{2}, \quad Q = \frac{d\epsilon}{\cos(\pi/(n+1))}$$
 (26)

Then we can solve for the eigenvalue  $\hat{E}$  of the scaled Hamiltonian of Eq. 21 as

$$\hat{E}(n, d\epsilon) = 2 - \cos(\pi/(n+1)) \left( f^2 + (1/f)^2 \right) \tag{27}$$

where  $f(d\epsilon)$  is given by Eq. 26.

We compute the normalization constant C for the eigenfunction, which satisfies

$$\sum_{k=1}^{n} \psi_k^2 = C^2 \tag{28}$$

so that  $\psi_k/C$  is properly normalized. This gives

$$C^{2} = (1/f)^{2} \sum_{k \text{ odd}} \sin(\pi k/(n+1))^{2} + f^{2} \sum_{k \text{ even}} \sin(\pi k/(n+1))^{2}$$
(29)

Both sums can be evaluated analytically, and both equal (n+1)/4, so we have

$$C^{2} = \left(f^{2} + (1/f)^{2}\right) \frac{n+1}{4} \tag{30}$$

Fig. 25 shows that our analytical solution for the eigenfunctions agrees precisely with numerical results for the Hamiltonian of Eq. 21.

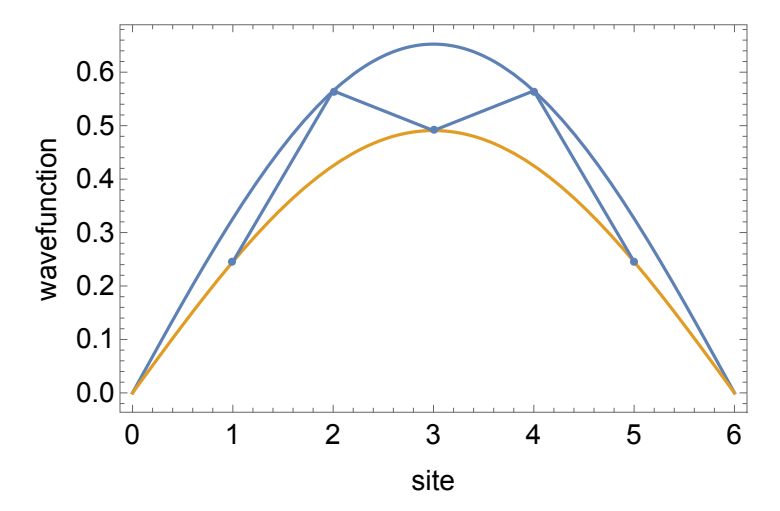


Figure 25: The alternating co-oligomer bonding wavefunction for a pentamer with  $d\epsilon = 0.5$  jumps on adjacent sites between two sinusoidal envelopes.

We can undo the scaling we did to simplify the algebra above, writing the eigenvalue of the original Hamiltonian as

$$E(n, \epsilon, d\epsilon, t) = \epsilon - 2t + t\hat{E}(n, d\epsilon/2t)$$
(31)

where the two onsite energies are  $\epsilon \pm d\epsilon$  and the hopping matrix element between them is t.

# References

- [1] Tejasvini Sharma, Prerna Mahajan, Mohammad Adil Afroz, Anupriya Singh, Yukta, Naveen Kumar Tailor, Smruti Purohit, Sonali Verma, Bhavya Padha, Vinay Gupta, Sandeep Arya, and Soumitra Satapathi. Recent Progress in Advanced Organic Photovoltaics: Emerging Techniques and Materials. ChemSusChem, 15(5):e202101067, 3 2022. ISSN 1864564X. doi: 10.1002/cssc.202101067.
- [2] Sarah Holliday, Raja Shahid Ashraf, Andrew Wadsworth, Derya Baran, Syeda Amber Yousaf, Christian B. Nielsen, Ching Hong Tan, Stoichko D. Dimitrov, Zhengrong Shang, Nicola Gasparini, Maha Alamoudi, Frédéric Laquai, Christoph J. Brabec, Alberto Salleo, James R. Durrant, and Iain McCulloch. High-efficiency and air-stable P3HT-based polymer solar cells with a new non-fullerene acceptor. Nature Communications, 7, 6 2016. ISSN 20411723. doi: 10.1038/ncomms11585.
- [3] Hyojung Cha, Jiaying Wu, Andrew Wadsworth, Jade Nagitta, Saurav Limbu, Sebastian Pont, Zhe Li,

- Justin Searle, Mark F. Wyatt, Derya Baran, Ji Seon Kim, Iain McCulloch, and James R. Durrant. An Efficient, "Burn in" Free Organic Solar Cell Employing a Nonfullerene Electron Acceptor. *Advanced Materials*, 29(33):1–8, 2017. ISSN 15214095. doi: 10.1002/adma.201701156.
- [4] Derya Baran, Raja Shahid Ashraf, David A. Hanifi, Maged Abdelsamie, Nicola Gasparini, Jason A. Röhr, Sarah Holliday, Andrew Wadsworth, Sarah Lockett, Marios Neophytou, Christopher J.M. Emmott, Jenny Nelson, Christoph J. Brabec, Aram Amassian, Alberto Salleo, Thomas Kirchartz, James R. Durrant, and Iain McCulloch. Reducing the efficiency-stability-cost gap of organic photovoltaics with highly efficient and stable small molecule acceptor ternary solar cells. *Nature Materials*, 16(3):363–369, 2017. ISSN 14764660. doi: 10.1038/nmat4797.
- [5] Cenqi Yan, Stephen Barlow, Zhaohui Wang, He Yan, Alex K.Y. Jen, Seth R. Marder, and Xiaowei Zhan. Non-fullerene acceptors for organic solar cells. *Nature Reviews Materials*, 3, 2018. ISSN 20588437. doi: 10.1038/natrevmats.2018.3.
- [6] Jun Yuan, Yunqiang Zhang, Liuyang Zhou, Guichuan Zhang, Hin Lap Yip, Tsz Ki Lau, Xinhui Lu, Can Zhu, Hongjian Peng, Paul A. Johnson, Mario Leclerc, Yong Cao, Jacek Ulanski, Yongfang Li, and Yingping Zou. Single-Junction Organic Solar Cell with over 15% Efficiency Using Fused-Ring Acceptor with Electron-Deficient Core. Joule, 3(4):1140–1151, 2019. ISSN 25424351. doi: 10.1016/j.joule.2019.01.004. URL https://doi.org/10.1016/j.joule.2019.01.004.
- [7] Ardalan Armin, Wei Li, Oskar J. Sandberg, Zuo Xiao, Liming Ding, Jenny Nelson, Dieter Neher, Koen Vandewal, Safa Shoaee, Tao Wang, Harald Ade, Thomas Heumüller, Christoph Brabec, and Paul Meredith. A History and Perspective of Non-Fullerene Electron Acceptors for Organic Solar Cells. Advanced Energy Materials, 11(15):1–42, 2021. ISSN 16146840. doi: 10.1002/aenm.202003570.
- [8] Lei Zhu, Ming Zhang, Wenkai Zhong, Shifeng Leng, Guanqing Zhou, Yecheng Zou, Xuan Su, Han Ding, Peiyang Gu, Feng Liu, and Yongming Zhang. Progress and prospects of the morphology of non-fullerene acceptor based high-efficiency organic solar cells. *Energy and Environmental Science*, 14(8):4341–4357, 8 2021. ISSN 17545706. doi: 10.1039/dlee01220g.
- [9] Xiangjian Wan, Chenxi Li, Mingtao Zhang, and Yongsheng Chen. Acceptor-donor-acceptor type molecules for high performance organic photovoltaics-chemistry and mechanism. *Chemical Society Re*views, 49(9):2828–2842, 5 2020. ISSN 14604744. doi: 10.1039/d0cs00084a.
- [10] Hugo Bronstein, Christian B. Nielsen, Bob C. Schroeder, and Iain McCulloch. The role of chemical

- design in the performance of organic semiconductors. Nature Reviews Chemistry, 4(2):66–77, 2020. ISSN 23973358. doi: 10.1038/s41570-019-0152-9.
- [11] Kangkang Weng, Linglong Ye, Lei Zhu, Jinqiu Xu, Jiajia Zhou, Xiang Feng, Guanghao Lu, Songting Tan, Feng Liu, and Yanming Sun. Optimized active layer morphology toward efficient and polymer batch insensitive organic solar cells. *Nature Communications*, 11(1):1–9, 6 2020. ISSN 20411723. doi: 10.1038/s41467-020-16621-x. URL https://www.nature.com/articles/s41467-020-16621-x.
- [12] Surya Subianto, Mats Andersson, Naba Dutta, and Namita Roy Choudhury. Novel rhodanine based molecular acceptor for organic solar cells. EPJ Photovoltaics, 8, 2017. ISSN 21050716. doi: 10.1051/epjpv/2017007.
- [13] Yongxi Li, Minchao Gu, Zhe Pan, Bin Zhang, Xutong Yang, Junwei Gu, and Yu Chen. Indacenodithiophene: A promising building block for high performance polymer solar cells. *Journal of Materials Chemistry A*, 5(22):10798–10814, 2017. ISSN 20507496. doi: 10.1039/c7ta02562a.
- [14] Francis Lin, Kui Jiang, Werner Kaminsky, Zonglong Zhu, and Alex K.Y. Jen. A Non-fullerene Acceptor with Enhanced Intermolecular π-Core Interaction for High-Performance Organic Solar Cells. Journal of the American Chemical Society, 142(36):15246–15251, 9 2020. ISSN 15205126. doi: 10.1021/jacs.0c07083. URL https://pubs.acs.org/doi/full/10.1021/jacs.0c07083.
- [15] Wei Liu, Xiang Xu, Jun Yuan, Mario Leclerc, Yingping Zou, and Yongfang Li. Low-Bandgap Non-fullerene Acceptors Enabling High-Performance Organic Solar Cells. *ACS Energy Letters*, 6(2):598–608, 2021. ISSN 23808195. doi: 10.1021/acsenergylett.0c02384. URL http://pubs.acs.org/journal/aelccp.
- [16] Zhi Wen Zhao, Omer H. Omar, Daniele Padula, Yun Geng, and Alessandro Troisi. Computational Identification of Novel Families of Nonfullerene Acceptors by Modification of Known Compounds. *Journal of Physical Chemistry Letters*, 12(20):5009–5015, 2021. ISSN 19487185. doi: 10.1021/acs.jpclett.1c01010.
- [17] Rex Manurung, Ping Li, and Alessandro Troisi. Rapid Method for Calculating the Conformationally Averaged Electronic Structure of Conjugated Polymers. *Journal of Physical Chemistry B*, 125(23): 6338–6348, 2021. ISSN 15205207. doi: 10.1021/acs.jpcb.1c02866.
- [18] Joel H. Bombile, Michael J. Janik, and Scott T. Milner. Tight binding model of conformational disorder effects on the optical absorption spectrum of polythiophenes. *Physical Chemistry*

- Chemical Physics, 18(18):12521-12533, 2016. ISSN 14639076. doi: 10.1039/c6cp00832a. URL http://dx.doi.org/10.1039/C6CP00832A.
- [19] David P. McMahon and Alessandro Troisi. An ad hoc tight binding method to study the electronic structure of semiconducting polymers. Chemical Physics Letters, 480(4-6):210-214, 2009. ISSN 00092614. doi: 10.1016/j.cplett.2009.09.032. URL http://dx.doi.org/10.1016/j.cplett.2009.09.032.
- [20] Joel H. Bombile, Michael J. Janik, and Scott T. Milner. Energetics of exciton binding and dissociation in polythiophenes: A tight binding approach. *Physical Chemistry Chemical Physics*, 21(22):11999–12011, 2019. ISSN 14639076. doi: 10.1039/c9cp01116a.
- [21] Joel H. Bombile, Michael J. Janik, and Scott T. Milner. Polaron formation mechanisms in conjugated polymers. *Physical Chemistry Chemical Physics*, 20(1):317–331, 2017. ISSN 14639076. doi: 10.1039/c7cp04355d. URL http://dx.doi.org/10.1039/C7CP04355D.
- [22] Joel H. Bombile, Shreya Shetty, Michael J. Janik, and Scott T. Milner. Polaron hopping barriers and rates in semiconducting polymers. *Physical Chemistry Chemical Physics*, 22(7):4032–4042, 2020. ISSN 14639076. doi: 10.1039/c9cp06039a.
- [23] Prithvi Tipirneni, Vishal Jindal, Michael J. Janik, and Scott T. Milner. Tight binding models accurately predict band structures for copolymer semiconductors. *Physical Chemistry Chemical Physics*, 22(35): 19659–19671, 2020. ISSN 14639076. doi: 10.1039/d0cp01833c.
- [24] Liam Wilbraham, Enrico Berardo, Lukas Turcani, Kim E. Jelfs, and Martijn A. Zwijnenburg. High-Throughput Screening Approach for the Optoelectronic Properties of Conjugated Polymers. Journal of Chemical Information and Modeling, 58(12):2450-2459, 12 2018. ISSN 1549960X. doi: 10.1021/acs.jcim.8b00256. URL https://pubs.acs.org/doi/full/10.1021/acs.jcim.8b00256.
- [25] Anders S. Christensen, Tomáš Kubař, Qiang Cui, and Marcus Elstner. Semiempirical Quantum Mechanical Methods for Noncovalent Interactions for Chemical and Biochemical Applications. Chemical Reviews, 116(9):5301–5337, 2016. ISSN 15206890. doi: 10.1021/acs.chemrev.5b00584.
- [26] Stefan Grimme, Christoph Bannwarth, and Philip Shushkov. A Robust and Accurate Tight-Binding Quantum Chemical Method for Structures, Vibrational Frequencies, and Noncovalent Interactions of Large Molecular Systems Parametrized for All spd-Block Elements (Z = 1-86). Journal of Chemical Theory and Computation, 13(5):1989–2009, 5 2017. ISSN 15499626. doi: 10.1021/acs.jctc.7b00118. URL https://pubs.acs.org/doi/full/10.1021/acs.jctc.7b00118.

- [27] Christoph Bannwarth, Sebastian Ehlert, and Stefan Grimme. GFN2-xTB An Accurate and Broadly Parametrized Self-Consistent Tight-Binding Quantum Chemical Method with Multipole Electrostatics and Density-Dependent Dispersion Contributions. *Journal of Chemical Theory and Computation*, 15 (3):1652–1671, 2019. ISSN 15499626. doi: 10.1021/acs.jctc.8b01176.
- [28] Christoph Bannwarth, Eike Caldeweyher, Sebastian Ehlert, Andreas Hansen, Philipp Pracht, Jakob Seibert, Sebastian Spicher, and Stefan Grimme. Extended tight-binding quantum chemistry methods. Wiley Interdisciplinary Reviews: Computational Molecular Science, 11(2):1–49, 2021. ISSN 17590884. doi: 10.1002/wcms.1493.
- [29] Gekko Budiutama, Ruicheng Li, Sergei Manzhos, and Manabu Ihara. Hybrid Density Functional Tight Binding (DFTB)Molecular Mechanics Approach for a Low-Cost Expansion of DFTB Applicability. *Journal of Chemical Theory and Computation*, 19(15):5189–5198, 2023. ISSN 15499626. doi: 10.1021/acs.jctc.3c00310.
- [30] Puja Agarwala, Enrique D. Gomez, and Scott T. Milner. Fast, Faithful Simulations of Donor-Acceptor Interface Morphology. *Journal of Chemical Theory and Computation*, 18(11):6932-6939, 11 2022. ISSN 15499626. doi: 10.1021/acs.jctc.2c00470. URL https://pubs.acs.org/doi/abs/10.1021/acs.jctc.2c00470.
- [31] Murat Mesta, Jin Hyun Chang, Suranjan Shil, Kristian S. Thygesen, and Juan Maria Garcia Lastra. A Protocol for Fast Prediction of Electronic and Optical Properties of Donor-Acceptor Polymers Using Density Functional Theory and the Tight-Binding Method. *Journal of Physical Chemistry A*, 123(23): 4980–4989, 2019. ISSN 15205215. doi: 10.1021/acs.jpca.9b02391.
- [32] Shane Donaher, Puja Agarwala, and Scott T. Milner. A simple approach to hopping matrix elements between nearby molecules. 12 2022. URL http://arxiv.org/abs/2212.11831.
- [33] Axel D. Becke. Density-functional thermochemistry. III. The role of exact exchange. The Journal of Chemical Physics, 98(7):5648–5652, 8 1993. ISSN 00219606. doi: 10.1063/1.464913. URL https://aip.scitation.org/doi/abs/10.1063/1.464913.
- [34] Chengteh Lee, Weitao Yang, and Robert G. Parr. Development of the Colle-Salvetti correlation-energy formula into a functional of the electron density. *Physical Review B*, 37(2):785–789, 1 1988. ISSN 01631829. doi: 10.1103/PhysRevB.37.785. URL https://journals.aps.org/prb/abstract/10.1103/PhysRevB.37.785.

- [35] S. H. Vosko, L. Wilk, and M. Nusair. Accurate spin-dependent electron liquid correlation energies for local spin density calculations: a critical analysis. *Canadian Journal of Physics*, 58(8):1200–1211, 1980. ISSN 0008-4204. doi: 10.1139/p80-159.
- [36] P. J. Stephens, F. J. Devlin, C. F. Chabalowski, and M. J. Frisch. Ab Initio calculation of vibrational absorption and circular dichroism spectra using density functional force fields. *Journal of Physical Chemistry®*, 98(45):11623–11627, 1994. ISSN 00223654. doi: 10.1021/j100096a001. URL https://pubs.acs.org/doi/pdf/10.1021/j100096a001.
- [37] Qianqian Zhang, Mary Allison Kelly, Nicole Bauer, and Wei You. The Curious Case of Fluorination of Conjugated Polymers for Solar Cells. *Accounts of Chemical Research*, 50(9):2401–2409, 9 2017. ISSN 15204898. doi: 10.1021/acs.accounts.7b00326. URL https://pubs.acs.org/doi/full/10.1021/acs.accounts.7b00326.
- [38] Brandon H. Smith, Qianqian Zhang, Mary Allison Kelly, Joshua H. Litofsky, Dinesh Kumar, Alexander Hexemer, Wei You, and Enrique D. Gomez. Fluorination of Donor-Acceptor Copolymer Active Layers Enhances Charge Mobilities in Thin-Film Transistors. ACS Macro Letters, 6(10):1162–1167, 2017. ISSN 21611653. doi: 10.1021/acsmacrolett.7b00716.
- [39] Mary Allison Kelly, Steffen Roland, Qianqian Zhang, Youngmin Lee, Bernd Kabius, Qing Wang, Enrique D. Gomez, Dieter Neher, and Wei You. Incorporating Fluorine Substitution into Conjugated Polymers for Solar Cells: Three Different Means, Same Results. *Journal of Physical Chemistry C*, 121 (4):2059–2068, 2017. ISSN 19327455. doi: 10.1021/acs.jpcc.6b10993.
- [40] Jiyoul Lee. Comment on "investigation of the device instability feature caused by electron trapping in pentacene field effect transistors" [Appl. Phys. Lett. 100, 063306 (2012)]. Applied Physics Letters, 103 (3):2012–2014, 2013. ISSN 00036951. doi: 10.1063/1.4816013.